Final Report of the Consulting Contract for an Energy-Efficient and Sustainable Design of the Consalud's new Headquarters Building in Santiago de Chile

DIPARTIMENTO DI SCIENZE E TECNICHE PER I PROCESSI DI INSEDIAMENTO
DEPARTMENT OF ENVIRONMENTAL SCIENCES AND TECHNOLOGY

CONSALUD's NEW HEADQUARTERS BUILDING
SANTIAGO DE CHILE

Consulting Contract for an Energy Efficient and Sustainable Design

FINAL REPORT

Prof. Arch. Mario Grosso

Torino, Italy, December 3, 1998

Viale Mattioli 39, 10125 TORINO, ITALY Ph. ++39 11 564-4376 FAX: 011 564-4374 E-mail: grosso@araxp.polito.it

CONTENTS

INTRODUCTION

The following report is related to the energy and environmental consulting work on the bioclimatic design of Consalud's Headquarters Building in Santiago de Chile, commissioned to the Environmental Science and Technology Department, Polytechnic University of Turin, Italy, under the responsibility of professor Mario Grosso.

Main objective of the work is to contribute to the construction of a bioclimatic building requiring a minimum consumption of non-renewable energy, employing environmentally friendly and sustainable technologies, innovative for the Chilean reality, and leading to a better and more productive working environment.

The work was carried out through a continuing interactive process involving the design team and the consultants. It is schematically divided in the following phases:

- On-site concept design workshop, within which the following tasks were performed:

Qualitative evaluation of the general building forms and orientation with respect to solar and wind exposure as well as analysis of alternative typological configurations (atrium building and linear building) in terms of indoor comfort conditions.

Indications for envelope and structure aimed to minimising energy needs while improving thermal, visual and acoustic comfort.

Preliminary estimate of the thermal performance of a sample zone (first floor) of the NE wing (office spaces), based on average monthly meteorological data from the Santiago Airport.

Outline and preliminary performance evaluation of sustainable environmental control schemes such as shading devices, passive cooling with buried pipes, evaporative cooling, solar PV electrical and thermal combined systems.

- General bioclimatic design definition, comprising the following actions:

Definition of reference local climate conditions.

Sensitivity analyses of orientation and solar control effectiveness of the shading devices proposed, for the chosen building configuration.

Bioclimatic assessment of the principal designers' options related to construction technologies (building envelope and structure).

Thermal performance zone analysis of the NE wing for a reference basic configuration (free running).

- Schematic design of a passive-integrated HVAC system for the NE wing, comprising:

Integrated ventilation schemes based on active solar pre-heating and hybrid passive cooling systems.

Natural cooling through buried pipes.

Night ventilation of floor slabs.

- Assessment of energy savings for the various bioclimatic strategies (NE wing):

Solar control

Glazing

Cooling by night ventilation

Cooling by ventilation through buried pipes

Solar space pre-heating

Combined strategies

- Indications of bioclimatic design strategies for the SW wing (collective use spaces and call centre)

PART I – GENERAL ASPECTS

1 Local Climate Characterisation

Comfort and thermal analyses of passively climatised buildings require hourly meteorological data of at least a typical day for each month of the year, averaged over a 10 year-minimum period. Monthly values averaged over 10 ÷ 30 years are available at the moment for Pudahuell, the station closest to the construction site, but not hourly based. Therefore, mean monthly 24-hours profiles have been developed within the present consulting activity according to the procedures specified hereafter.

1.1 Available Meteorological Data

Available meteorological data averaged over about 10 years for Pudahuell are:

- daily global solar radiation;
- three-hour air temperature, relative humidity, wind velocity and direction and sky cover (at standard time hours 8, 14 and 20);
- average and absolute minimum air temperatures, average mean air temperatures, average and absolute maximum air temperatures;
- other data, such as the barometric pressure, the precipitation rates and some statistical analyses on days with data far from the mean ones, that are not particularly relevant for the work described in the present report.

Furthermore, for the same station of Pudahuell, long term data of mean monthly minimum and maximum air temperatures are available (data since 1968, available through the "Dirección Meteorologica de Chile").

Input data used for developing the 24-hours profiles are reported in Table 1, 2, 3, and 4.

Table 1 – Monthly averages of maximum air temperatures

Maximum air temperature [°C]								
	Average 1968/90	1991	1992	1993	1994	1995	1996	**Average 1968/96**
January	29.8	30.7	30.6	30.2	29.5	29.7	28.7	**29.8**
February	29.4	31.1	29.2	29.3	29.1	28.3	29.6	**29.4**
March	27.1	27.6	27.2	28.7	27.1	27.3	27.8	**27.2**
April	23.2	23.5	21.1	21.4	23.3	24.0	20.9	**23.0**
May	18.3	19.9	16.0	15.5	18.8	21.7	18.8	**18.3**
June	14.9	15.9	12.7	15.2	15.6	16.6	15.7	**15.0**
July	14.7	14.0	12.3	13.4	13.9	13.1	17.1	**14.5**
August	16.4	15.3	17.1	17.7	15.8	15.6	16.5	**16.4**
September	18.7	19.7	18.7	18.5	20.2	19.1	20.5	**18.9**
October	22.2	22.5	23.0	21.8	21.9	23.1	22.6	**22.3**
November	25.8	25.7	24.9	25.6	26.2	25.5	27.5	**25.8**
December	28.6	26.9	28.0	28.6	28.9	28.6	28.4	**28.5**

Table 2 – Monthly averages of minimum air temperatures

Minimum air temperature [°C]								
	Average 1968/90	1991	1992	1993	1994	1995	1996	**Average 1968/96**
January	11.5	9.7	12.1	12.4	11.9	12.0	11.4	**11.5**
February	10.8	10.1	11.0	12.3	10.5	11.3	10.5	**10.8**
March	8.9	9.3	10.7	10.3	9.8	9.3	10.0	**9.1**
April	6	8.0	7.6	8.4	8.1	7.8	6.0	**6.3**
May	4.6	7.1	6.5	4.4	4.5	4.8	3.2	**4.7**
June	2.7	4.6	3.7	4.4	4.5	4.9	1.5	**3.0**
July	2.5	3.3	1.8	0.3	3.0	2.3	2.8	**2.4**
August	3.4	1.6	3.4	1.5	1.9	2.1	3.6	**3.2**
September	4.7	6.3	5.2	3.7	6.5	5.9	4.3	**4.8**
October	6.7	5.5	7.0	6.7	7.2	6.8	7.2	**6.7**
November	8.6	9.1	9.4	7.6	9.3	9.5	9.4	**8.7**
December	10.4	10.5	10.2	10.7	11.7	11.7	10.7	**10.5**

Table 3 – Monthly averages of global daily solar radiation on horizontal plane

Global daily solar radiation [Wh/m^2]										
	1988	1989	1990	1991	1992	1993	1994	1995	1996	**Average 1988/96**
January	8299	8143	8284	8161	8067	7730	7658	7523	-	**7983**
February	6943	7507	7101	7448	6743	6765	6955	6715	7695	**7097**
March	5732	6025	5730	5540	5229	5698	5805	5661	5792	**5690**
April	4256	3930	3741	3632	3438	3103	3654	3889	3624	**3696**
May	2527	2320	2777	2003	2015	2331	2603	2796	-	**2422**
June	2027	1661	2285	2007	1649	1918	1882	1861	-	**1911**
July	2431	2413	2527	2023	2014	2351	1918	2006	-	**2210**
August	3095	2781	3101	2929	3028	3309	3110	3100	3217	**3074**
September	4830	4040	3845	3927	4668	-	3668	4384	4593	**4244**
October	6611	5903	5646	5936	6212	5481	5576	5999	6025	**5932**
November	7688	7320	7728	6644	6603	7573	7338	7308	7688	**7321**
December	8669	8493	7871	6617	8005	-	7862	8059	8304	**7985**

Table 4a – Monthly averages of air temperature at standard time hours 8, 14,20

Air temperature [°C]													
Year	Hour	Jan.	Feb.	March	April	May	June	July	Aug.	Sept.	Oct.	Nov.	Dec.
1987	8	16.5	15.5	13.1	7.9	5.9	3.7	4.9	5.9	7.5	11.6	15.3	16.8
	14	28.8	28.7	26.5	22.1	15	15.7	12.2	13.5	16	20.4	25.9	27.7
	20	23.6	23.4	21.4	16.7	11.1	10.4	9.4	10.9	12.7	15.8	19.8	22.6
1988	8	15.9	14.6	11.7	7.6	3	2	2.3	3.9	5.4	10.4	14.1	16.2
	14	28.1	28.7	25.9	22.6	17.3	14.6	13.4	15.3	17.5	23.3	26.3	28
	20	22.4	22.8	20.3	16.3	11.6	9.1	8.6	10.6	12.3	17.1	20	21.6
1989	8	16.7	15.4	10.9	8.2	4.7	2.9	2.4	5.6	7	10.5	16.4	17.3
	14	29.5	29.8	26.6	22.7	16.6	15.3	14.2	14.6	16.8	22.2	26.4	28.6
	20	23.6	24	19.7	16.1	10.7	9	8.5	10.5	11.5	14.6	18.9	21.4
1990	8	17	14.2	10.7	8.3	3.4	1.8	1	4.9	7.9	10.2	13.9	16.4
	14	30.3	27.7	26.5	21.5	18.4	17.2	14.3	17.2	17.5	20.8	26.2	27.9
	20	23.2	21.5	19.3	15.3	11.2	9.4	7.9	11.5	12.4	14.5	18.2	21.3
1991	8	16.4	14.8	11.9	9.3	8.2	5.5	4.2	2.9	8.4	10	13.6	15.9
	14	29.5	29.8	26	22.2	18.6	14.6	12.9	14	18.	21.2	24.4	25.6
	20	22.7	22.6	19.4	16.2	13.7	9.9	8.6	9.1	13.5	14.8	17.8	19.6
1992	8	16.9	14.3	12.7	8.5	7.2	4.2	2.8	4.2	6.8	10.6	13.5	16.2
	14	29.3	27.5	25.7	19.8	14.7	11.5	10.9	15.4	17.2	21.8	23.6	26.8
	20	23.1	21.2	20.4	15.3	11.7	8.9	7.5	10.8	12.9	16.2	18	21
1993	8	17.1	15.4	12.3	9.4	5.1	5.6	1.4	2.5	5.2	10.3	13.8	15.8
	14	28.7	27.9	27.3	20.1	14.4	13.9	12.1	16.3	17.3	20.8	24.6	27.4
	20	23.6	22.5	21.6	16.2	10.6	10.1	7.6	11.3	12.8	15.6	18.6	21.7
1994	8	16.1	13.6	11.8	8.9	5.3	5.6	3.6	2.8	8.4	10.6	14.2	16.9
	14	28.3	27.8	25.8	22.1	17.8	14.3	12.9	14.6	18.7	20.9	25.5	27.8
	20	22.6	21.7	19.6	17.1	12.8	10.6	9	10.5	14.3	16.1	19.4	22.6
1995	8	16.6	14.2	11.4	8.9	5.8	5.4	3.2	3	7.5	10.4	14	16
	14	28.5	27	25.9	22.6	20.3	15.5	11.3	14.1	18	22	24.3	27.6
	20	23.6	21.6	20.5	17.4	14.6	11.5	8.6	10.5	13.4	16.4	18.5	21.4
1996	8	16	14.6	12	6.9	4.1	2.6	3.4	4.5	5.8	10.9	15.4	16.6
	14	27.6	28.7	26.6	19.5	17.4	14.6	15.6	15.1	19	21.6	26.4	27.3
	20	22	22.6	20.8	15.2	12	9.8	10.8	11.1	13.9	16.2	20.4	21.8

Table 4b – Monthly averages of relative humidity at standard time hours 8, 14, and 20

Relative humidity [%]													
Year	Hour	Jan.	Feb.	March	April	May	June	July	Aug.	Sept.	Oct.	Nov.	Dec.
1987	8	75	80	88	89	94	95	95	94	92	90	77	67
	14	39	39	46	45	63	60	75	69	64	58	42	35
	20	50	51	60	63	81	79	85	82	76	72	56	43
1988	8	73	85	89	91	90	90	92	93	92	79	75	69
	14	36	39	41	43	47	53	59	56	49	34	34	33
	20	47	53	57	62	67	73	76	77	68	51	50	47
1989	8	72	76	86	91	97	96	96	97	96	90	75	71
	14	34	34	36	46	63	63	60	71	65	48	40	36
	20	46	45	52	65	87	84	83	88	85	70	56	49
1990	8	68	83	86	93	93	90	95	95	93	90	76	66
	14	33	41	35	51	48	48	59	59	59	49	35	32
	20	43	54	53	71	72	72	79	79	78	69	53	44
1991	8	67	78	89	92	94	96	97	97	96	89	82	73
	14	31	31	45	50	62	69	74	70	64	48	44	42
	20	41	45	61	70	80	89	90	89	81	70	62	55
1992	8	79	81	91	94	97	96	97	97	96	86	80	66
	14	39	39	44	52	67	77	74	59	58	45	43	37
	20	51	54	60	66	83	87	87	80	75	63	60	47
1993	8	67	79	89	95	98	97	97	96	94	82	69	68
	14	35	39	37	59	65	73	64	51	46	42	31	31
	20	44	52	51	73	83	88	83	70	66	59	46	44
1994	8	73	79	88	88	95	99	96	92	87	82	70	65
	14	33	31	37	43	55	70	69	55	50	41	32	30
	20	46	44	56	58	76	86	86	70	65	57	46	40
1995	8	61	76	80	86	91	92	92	95	92	81	75	80
	14	28	33	33	40	42	57	60	55	53	39	41	38
	20	36	46	45	59	64	77	74	71	71	54	55	56
1996	8	67	74	86	95	94	90	97	97	85	76	54	53
	14	32	29	38	50	51	54	59	61	39	36	27	28
	20	45	42	52	66	71	73	77	79	53	50	37	37

1.2 Calculated Monthly 24-hour Profiles

Based on those values, monthly 24-hour profiles for temperature, solar radiation, both direct and diffuse, and relative humidity were developed using the following procedures:
ASHRAE stabilised sinusoidal periodic method for air temperature ([1]);
Kusuda - Ishii's method for solar radiation ([2]);
Fitting method for relative humidity.

As Tables 1 and 2 show, the very long term available data source (from 1968 to 1996) used for developing the air temperature 24-hours profiles make the results of calculation quite reliable. Shorter time data sets are available for developing solar radiation 24-hours profiles (from 1988 to 1996 with some lacks in 1993 and 1996, see Table 3) as well as the relative humidity 24-hours

([1]) ASHRAE, *Handbook of Fundamentals*, 1981.
([2]) Kusuda T., and K. Ishii, *Hourly solar radiation data for vertical and horizontal surfaces on average days in the U.S. and Canada*, NBS Building, Science Series 96, Washington DC, 1977.

profiles (from 1987 to 1996, see Table 4b). However, the averaging period for these data is 9 – 10 years long. Hence, the results of calculation can be considered representative enough.

1.2.1 *Air temperature*

The procedure implemented for developing the air temperature 24-hours profiles (ASHRAE stabilised sinusoidal periodic method) is based on the assumption that the air temperature profile is sinusoidal for each mean monthly day. The profile is given by the sum of the average temperatures plus two sinusoidal perturbations: the main one having a 24 hours period and the minor one having a 12 hours period. Furthermore, it is assumed that the air temperature reaches its minimum just before the sunrise and its maximum 2 ÷ 3 hours after the sun culmination.

Table 5 – Calculated air temperature hourly profiles for a typical day of each month

Air temperature hourly profiles [°C]												
Standard time	Jan.	Feb.	March	April	May	June	July	Aug.	Sept.	Oct.	Nov.	Dec.
1	15.8	17.2	15.3	14.3	11.2	8.7	8.2	9.4	9.7	12.1	12.7	14.7
2	14.2	15.7	13.8	13.4	10.4	8.0	7.5	8.7	8.5	10.8	11.2	13.1
3	12.8	14.0	12.2	11.9	9.2	7.0	6.5	7.6	7.2	9.4	9.9	11.8
4	11.9	12.4	10.7	10.1	7.8	5.7	5.2	6.1	6.0	8.1	9.0	10.9
5	11.5	11.3	9.5	8.3	6.3	4.3	3.8	4.7	5.2	7.1	8.7	10.5
6	11.9	10.8	9.1	6.9	5.1	3.3	2.8	3.6	4.8	6.7	9.1	10.9
7	13.1	11.3	9.6	6.3	4.7	3.0	2.4	3.2	5.2	7.1	10.2	12.1
8	15.1	12.9	11.1	6.9	5.2	3.4	2.9	3.6	6.4	8.4	12.1	14.1
9	17.7	15.3	13.5	8.7	6.6	4.6	4.2	5.0	8.2	10.5	14.5	16.6
10	20.7	18.4	16.5	11.4	8.8	6.6	6.1	7.2	10.6	13.1	17.3	19.5
11	23.6	21.8	19.8	14.7	11.5	9.0	8.5	9.8	13.1	15.9	20.0	22.4
12	26.2	24.9	22.8	18.0	14.2	11.3	10.9	12.4	15.5	18.5	22.4	25.0
13	28.2	27.4	25.2	20.7	16.4	13.3	12.8	14.5	17.3	20.5	24.3	26.9
14	29.4	28.9	26.7	22.4	17.8	14.6	14.1	15.9	18.5	21.8	25.4	28.1
15	29.8	29.4	27.2	23.0	18.3	15.0	14.5	16.4	18.9	22.3	25.8	28.5
16	29.5	29.0	26.8	22.5	17.9	14.6	14.2	16.0	18.5	21.9	25.5	28.2
17	28.5	27.8	25.6	21.1	16.8	13.6	13.2	14.9	17.6	20.9	24.6	27.2
18	27.1	26.2	24.1	19.3	15.3	12.3	11.8	13.4	16.4	19.6	23.3	25.9
19	25.6	24.5	22.5	17.5	13.8	11.0	10.5	12.0	15.2	18.2	21.8	24.3
20	23.9	23.0	21.0	16.0	12.6	9.9	9.5	10.8	14.0	16.9	20.3	22.7
21	22.3	21.7	19.7	15.1	11.9	9.3	8.8	10.1	13.0	15.8	18.8	21.1
22	20.7	20.6	18.6	14.7	11.6	9.0	8.5	9.8	12.2	14.9	17.3	19.5
23	19.0	19.6	17.7	14.7	11.5	9.0	8.5	9.8	11.5	14.1	15.7	17.9
24	17.4	18.5	16.6	14.6	11.5	8.9	8.5	9.7	10.6	13.1	14.2	16.3

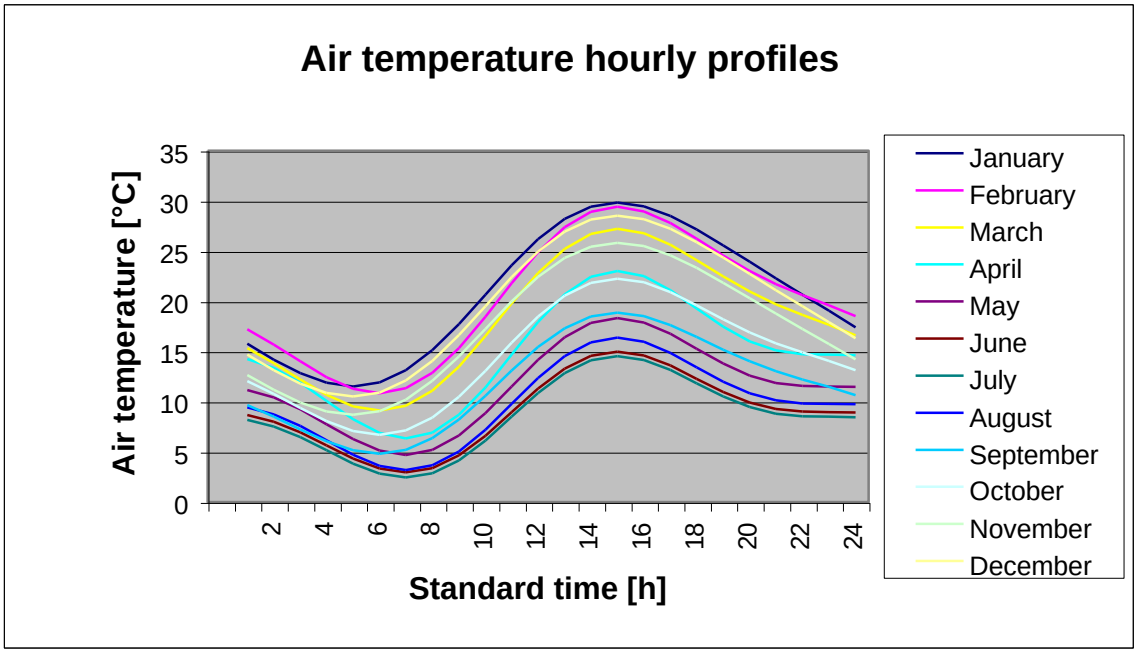

Fig. 1 – Calculated temperature hourly profiles for a typical day of each month

1.2.2 *Solar radiation*

The procedure implemented for developing the solar radiation 24-hours profiles was originally developed for calculating the solar radiation profiles of many sites in the U.S. and Canada (Kusuda, Ishii, 1977). Afterwards, it became probably the world mostly used procedure for elaborating solar radiation data. The great interest of this method is due to the possibility of developing solar radiation (both direct and diffuse) 24-hours profiles starting from one type of experimental data only (the global daily solar radiation on horizontal plane), in addition to geographical data of the site (latitude, longitude, etc.).

First of all, the procedure allows for calculating diffuse and direct contributions to the global daily solar radiation on horizontal plane. Secondly, diffuse and direct solar radiation 24-hours profiles can be developed. If global solar radiation 24-hours profiles are required, they can be obtained by adding up diffuse and direct solar radiation.

Table 6a – Calculated diffuse solar radiation hourly profiles on horizontal plane for a typical day of each month

Diffuse solar radiation hourly profiles [W/m^2]												
Standard time	Jan.	Feb.	March	April	May	June	July	Aug.	Sept.	Oct.	Nov.	Dec.
1	0	0	0	0	0	0	0	0	0	0	0	0
2	0	0	0	0	0	0	0	0	0	0	0	0
3	0	0	0	0	0	0	0	0	0	0	0	0
4	0	0	0	0	0	0	0	0	0	0	0	0
5	0	0	0	0	0	0	0	0	0	0	0	0
6	3	0	0	0	0	0	0	0	0	0	17	16
7	41	27	13	0	0	0	0	0	17	50	63	56
8	79	69	61	46	23	8	9	33	70	101	106	96
9	114	108	105	95	68	51	54	80	118	146	146	132
10	144	141	142	135	106	88	92	120	158	182	178	162
11	166	166	170	164	133	115	121	149	186	208	200	184
12	180	182	187	181	149	130	137	166	202	221	212	196
13	184	187	191	184	151	133	142	170	203	220	212	198
14	178	181	183	173	140	124	133	159	190	206	200	190
15	163	164	163	148	116	102	112	136	164	180	177	171
16	139	138	131	112	82	70	80	102	126	142	145	144
17	107	104	92	67	39	30	39	58	80	97	105	110
18	72	65	46	15	0	0	0	8	27	46	62	72
19	33	23	0	0	0	0	0	0	0	0	16	31
20	0	0	0	0	0	0	0	0	0	0	0	0
21	0	0	0	0	0	0	0	0	0	0	0	0
22	0	0	0	0	0	0	0	0	0	0	0	0
23	0	0	0	0	0	0	0	0	0	0	0	0
24	0	0	0	0	0	0	0	0	0	0	0	0

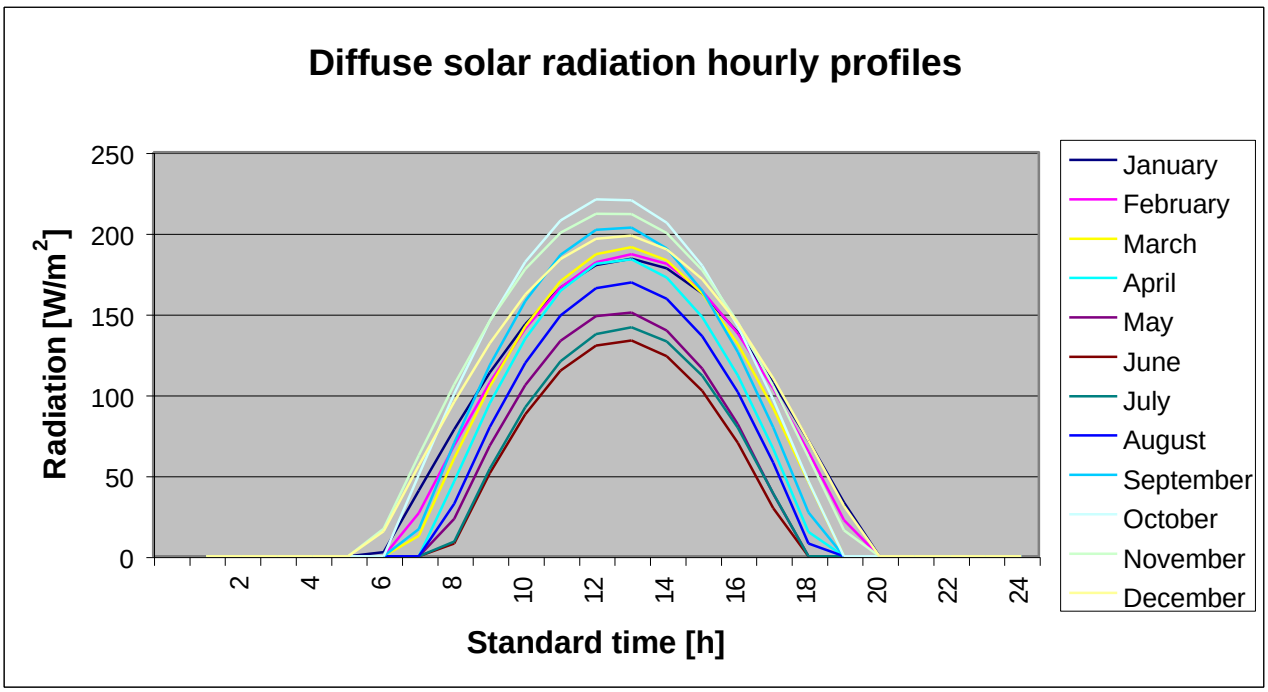

Fig. 2a – Calculated diffuse solar radiation hourly profiles on horizontal plane

for a typical day of each month

Table 6b – Calculated direct solar radiation hourly profiles on horizontal plane for a typical day of each month

Direct solar radiation hourly profiles [W/m^2]												
Standard time	Jan.	Feb.	March	April	May	June	July	Aug.	Sept.	Oct.	Nov.	Dec.
1	0	0	0	0	0	0	0	0	0	0	0	0
2	0	0	0	0	0	0	0	0	0	0	0	0
3	0	0	0	0	0	0	0	0	0	0	0	0
4	0	0	0	0	0	0	0	0	0	0	0	0
5	0	0	0	0	0	0	0	0	0	0	0	0
6	0	0	0	0	0	0	0	0	0	0	5	5
7	84	29	2	0	0	0	0	0	4	64	125	129
8	258	186	120	48	9	0	0	23	93	199	283	299
9	434	359	273	152	79	47	56	110	197	329	433	463
10	589	514	409	246	148	106	124	191	286	437	557	603
11	708	633	513	317	200	152	178	253	351	514	645	706
12	780	708	575	357	229	179	210	289	386	553	690	765
13	802	732	591	364	234	184	218	297	389	551	690	774
14	770	703	560	337	212	168	201	275	360	509	643	734
15	689	623	485	278	167	131	161	226	300	430	554	647
16	562	500	370	192	103	77	101	154	215	320	429	520
17	402	343	226	90	29	17	31	67	113	189	280	364
18	223	168	74	3	0	0	0	0	15	55	122	193
19	56	18	0	0	0	0	0	0	0	0	4	39
20	0	0	0	0	0	0	0	0	0	0	0	0
21	0	0	0	0	0	0	0	0	0	0	0	0
22	0	0	0	0	0	0	0	0	0	0	0	0
23	0	0	0	0	0	0	0	0	0	0	0	0
24	0	0	0	0	0	0	0	0	0	0	0	0

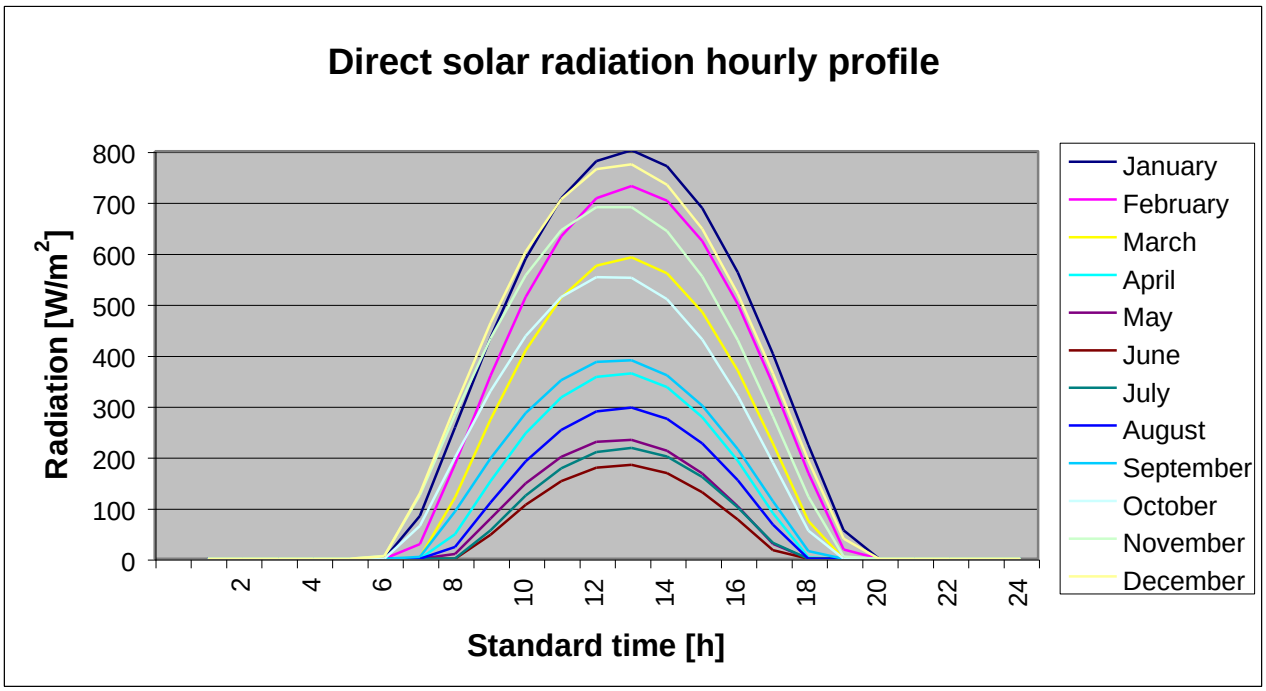

Fig. 2b – Calculated direct solar radiation hourly profiles on horizontal plane for a typical day of each month

Table 6c – Calculated global solar radiation hourly profiles on horizontal plane for a typical day of each month

Global solar radiation hourly profiles [W/m^2]												
Standard time	Jan.	Feb.	March	April	May	June	July	Aug.	Sept.	Oct.	Nov.	Dec.
1	0	0	0	0	0	0	0	0	0	0	0	0
2	0	0	0	0	0	0	0	0	0	0	0	0
3	0	0	0	0	0	0	0	0	0	0	0	0
4	0	0	0	0	0	0	0	0	0	0	0	0
5	0	0	0	0	0	0	0	0	0	0	0	0
6	3	0	0	0	0	0	0	0	0	0	23	21
7	125	56	15	0	0	0	0	0	21	115	188	185
8	336	254	181	95	32	8	10	56	163	300	389	394
9	548	467	378	247	147	99	110	190	315	475	578	595
10	733	655	551	381	254	194	216	311	444	619	734	765
11	874	800	683	481	333	267	298	402	537	722	845	890
12	960	890	762	538	378	310	347	455	588	774	902	961
13	986	918	783	548	384	318	359	466	593	772	902	973
14	949	884	744	509	352	292	334	434	550	716	843	924
15	851	788	647	426	283	233	272	362	465	610	731	819
16	701	638	501	304	185	147	181	256	342	462	574	665
17	510	447	318	156	68	46	70	125	193	286	385	474
18	295	233	120	18	0	0	0	8	42	102	183	264
19	89	41	0	0	0	0	0	0	0	0	20	70
20	0	0	0	0	0	0	0	0	0	0	0	0
21	0	0	0	0	0	0	0	0	0	0	0	0
22	0	0	0	0	0	0	0	0	0	0	0	0
23	0	0	0	0	0	0	0	0	0	0	0	0
24	0	0	0	0	0	0	0	0	0	0	0	0

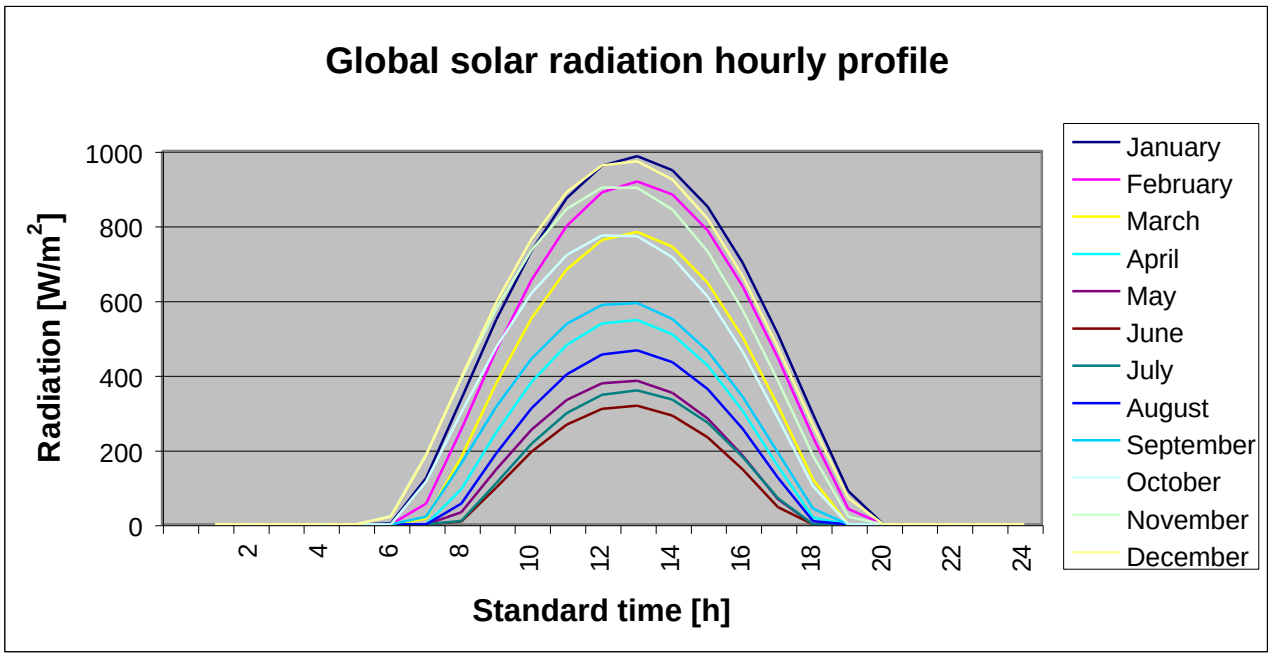

Fig. 2c – Calculated global solar radiation hourly profiles on horizontal plane for a typical day of each month

1.2.3 *Relative humidity*

The procedure implemented for developing the relative humidity 24-hours profiles (fitting method) is based on the experimental evidence that all over the world the relative humidity can be quite variable during a day, but the vapour partial pressure is almost constant, i.e., its variation takes days for occurring. Maximum oscillations of ± 10-20% during a day are reported in the majority of the world meteorological stations and analysis of experimental data confirms that Santiago meets this assumption. Hence, vapour partial pressure 24-hours profiles can be developed by a simple fitting procedure that has to be consistent with a qualitative evaluation of the site, which can be obtained from data of air temperature and relative humidity of a few hours during the day.

Calculation of relative humidity can be done by a simple ratio of the vapour partial pressure to the vapour saturation partial pressure.

The 24-hours profiles for each typical monthly day for Pudahuell, calculated on the basis of the above summarised procedures, are reported in Table 5, 6 and 7 for air temperature, solar radiation, and relative humidity, respectively. For an easier visualisation of the results, the same profiles are graphically reported in Figure 1, 2 and 3.

Table 7 – Calculated relative humidity hourly profiles for a typical day of each month

Relative humidity hourly profiles [%]												
Standard time	Jan.	Feb.	March	April	May	June	July	Aug.	Sept.	Oct.	Nov.	Dec.
1	69.0	65.2	68.9	66.1	70.6	78.0	75.7	74.3	77.1	70.1	72.7	66.4
2	75.6	71.3	74.8	69.0	72.9	80.0	77.7	76.5	81.4	75.0	78.9	72.3
3	81.8	78.7	81.9	74.1	76.8	83.2	80.9	80.3	86.4	80.8	84.8	77.8
4	86.6	86.4	89.2	81.1	82.0	87.4	85.0	85.2	91.4	86.6	89.3	82.0
5	88.4	92.7	95.1	88.8	87.5	91.7	89.3	90.5	95.2	91.3	91.0	83.6
6	86.4	95.2	97.5	95.3	92.0	95.1	92.7	94.7	96.7	93.2	89.1	81.8
7	80.4	92.4	94.8	97.9	93.8	96.4	94.0	96.3	95.0	91.1	83.5	76.5
8	71.6	84.2	87.1	95.0	91.8	95.0	92.5	94.5	90.0	85.0	75.1	68.7
9	61.7	72.8	76.2	87.0	86.2	90.7	88.3	89.2	82.5	76.2	65.6	59.8
10	52.4	60.8	64.6	75.9	78.1	84.3	82.0	81.6	73.9	66.5	56.5	51.3
11	44.7	50.4	54.3	64.7	69.5	77.1	74.8	73.2	65.7	57.5	48.9	44.2
12	38.9	42.5	46.4	55.3	61.8	70.4	68.2	65.6	59.0	50.4	43.0	38.8
13	35.0	37.2	41.0	48.6	56.0	65.2	63.0	59.9	54.2	45.5	39.1	35.1
14	32.9	34.3	38.0	44.8	52.6	62.0	59.9	56.5	51.4	42.7	36.9	33.1
15	32.2	33.4	37.1	43.5	51.5	61.0	58.9	55.4	50.5	41.8	36.2	32.5
16	32.8	34.2	37.9	44.6	52.5	61.9	59.8	56.4	51.3	42.6	36.8	33.0
17	34.5	36.4	40.2	47.6	55.2	64.4	62.2	59.1	53.4	44.7	38.5	34.6
18	37.0	39.5	43.4	51.9	58.9	67.8	65.6	62.8	56.4	47.7	41.1	37.0
19	40.2	43.3	47.2	56.6	62.9	71.4	69.1	66.7	59.7	51.2	44.4	40.0
20	43.9	47.1	51.0	60.7	66.2	74.3	72.0	70.0	63.0	54.6	48.1	43.4
21	48.0	50.6	54.5	63.4	68.4	76.2	73.9	72.2	65.9	57.7	52.1	47.2
22	52.4	53.8	57.7	64.5	69.3	77.0	74.7	73.1	68.5	60.5	56.5	51.3
23	57.3	56.9	60.8	64.7	69.5	77.1	74.8	73.2	70.9	63.2	61.4	55.8
24	62.9	60.6	64.3	64.9	69.6	77.2	74.9	73.3	73.7	66.2	66.7	60.8

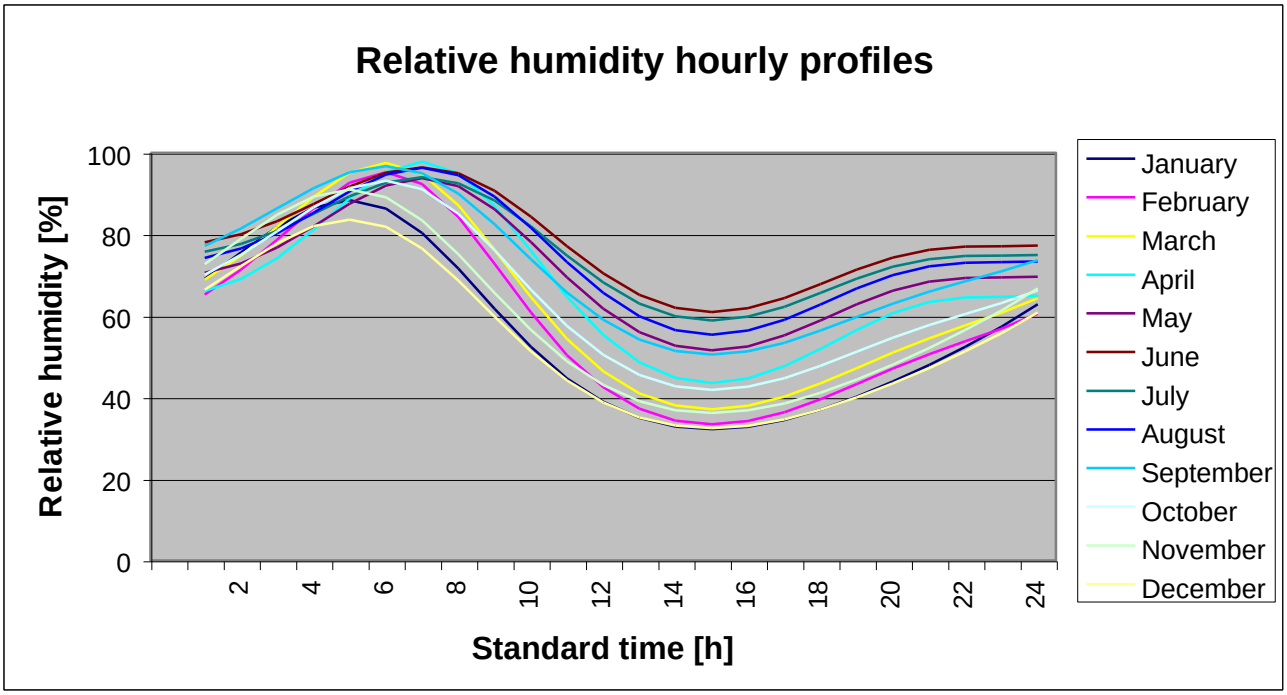

Fig. 3 – Calculated relative humidity hourly profiles for a typical day of each month

2 Building Form, Orientation, and Solar Control

2.1 Building Form

Three basic types of building form, indicated by the designers, were considered from a bioclimatic standpoint: linear, atrium, and courtyard.

Linear buildings, if sufficiently narrow, allows for a better optimisation of solar winter access and summer control as well as natural ventilation and daylighting. In addition, more floor surface than in the other types can be exposed to the same outdoor conditions.

Atrium buildings can utilise the glass-covered inner space as a buffer space in winter as well as an exhaust natural ventilation system in summer. Furthermore, the atrium space can become a winter garden enhancing the quality of connective and relation areas.

However, the atrium needs to be isolated from the working areas in order to avoid acoustic problems as well as flame and smoke propagation in case of fire, for which a careful design and operation of apertures in the glazed roof are needed (EEC, 1989). A risk of overheating needs also to be taken care of, particularly in a climate such as of Santiago, where the cooling season is roughly as long as the heating one.

Courtyard buildings are generally indicated for hot-dry climate locations (Olgyay, 1963) even if their actual thermal performance depends on several factors including size, courtyard dimensions and aspect ratios, surface treatment and presence of vegetation (Grosso, 1997). If properly designed, the courtyard space can generate differential daily cyclical radiative and convective conditions in relation to the outdoor climate, usable for natural ventilative cooling. In addition, inward roof slopes

can be conceived as rainwater recovery devices connected to an underground cistern, which in turn can be used as a heat sink.

As a drawback, a courtyard building is characterised by inner spaces of four different thermal behaviours depending on which of the side of the courtyard they are located. In a hypothetical orientation along the compass axes, in Santiago, the north side would have the best performance in winter, but could have overheating problems in summer due to the combined effects of high solar radiation and poor wind exposure.

Conversely, the well wind-exposed south wing might have a better thermal behaviour in summer than in winter, depending on the courtyard aspect ratios. For instance, in an E-W narrow rectangular plan courtyard with an overhanging roof the northward facade of the south wing could be almost completely shaded for all year and, therefore, get cool.

The east and west sides – particularly, the latter – could be affected by a combination of negative seasonal effects such as poor winter sun and summer wind exposures.

From the above considerations combined to other more general design requirements such as efficiency in circulation and space distribution, a choice toward a linear form was preferred after a wide range discussion during the on-site concept design workshop.

2.2 Orientation and Solar Control

The designers as a first choice depending on lot size and layout considerations chose an orientation of 30° clockwise from North for the whole complex. In addition, an overhanging *pergola* was foreseen on the northward and southward side of the roof of the NE wing, with a depth of 6.1 m and 5.2 m, respectively.

A sensitivity analysis on the thermal effect of orientation and overhang width was carried out through thermal simulation of a sample zone, the most exposed to solar radiation. The open space zone at the first floor, the least protected by the overhanging pergola, was chosen for simulation. Siting, form, and technology configurations are the ones delineated, in general terms, at the end of the concept design workshop and detailed later on. This simulation, as the others described below, has been carried out using the thermal model QUICKII (Mathews, 1986, 1989).

Three orientation angles were checked (0°, 15°, and 30° from North clockwise), with the above indicated overhang widths. The simulations were carried out assuming no climatisation and closed windows with only air infiltration, which satisfied the minimum air change required for indoor air quality both in summer and in winter. Set point indoor air temperatures of 20 °C and 26 °C for winter and summer, respectively, were chosen for load calculation.

The simulation results are shown in Table 8. As the table shows, increasing the azimuth angle from the due North towards East induces a slight increase in average annual indoor temperature, an increase in cooling annual energy and a decrease in heating energy. However, differing trends can be observed at each step. From 0° to 15°, the increase in average annual indoor temperature is meaningless (0.2 °C) as the increase in annual cooling energy (+ 1000 kWh over 48000 kWh), while yearly maximum indoor temperature, peak cooling loads as well as peak loads and annual energy for heating decrease. From 15° to 30°, heating loads and energy slightly lower but all other values increase, including a significant + 9000 kWh in annual cooling energy.

As a conclusion, a 15° East orientation seems to be the optimal one in terms of balancing heating and cooling. However, the 20° East orientation which came out as the minimum from South due to lot placement constraints is still a well performing configuration.

In the second series of simulation, the width of the overhanging pergola was increased of one meter at each step from the above mentioned values, keeping the orientation at 30° from North eastward (the worst among the previously analysed as far as cooling loads are concerned). As Table

8 shows, the advantage of increasing the overhang width is quite low both in terms of comfort and cooling loads. For each meter increase: – 0.05 °C in average annual indoor temperature, – 0.1 °C in maximum indoor temperature, – 0.25 kW in peak cooling loads, and – 1000 kWh in annual cooling energy. Heating loads and energy do not change.

Since those decreases do not offset the increase in costs due to the relevant higher widths, a 6-m width for both northward and southward pergola is suggested. If the East and West wall – the latter only at the upper floor – are also glazed, an all perimeter-overhanging roof would be preferable.

Table 8 – Results of the sensitivity analysis on orientation and overhangs

Orientation Angle [°]	Overhang Width [m]		Annual Indoor Temperature [°C]		Sensitive Peak Loads [kW]		Sensitive Annual Energy [kWh]	
	North	South	Average	Maximum	Cooling	Heating	Cooling	Heating
0	6.1	5.2	20.55	30.57	75.94	116.98	48000	56000
15	6.1	5.2	20.72	29.86	65.72	115.89	49000	54000
30	6.1	5.2	21.24	31.14	69.64	115.81	58000	53000
30	7.1	6.2	21.18	31.03	69.38	115.81	57000	53000
30	8.1	7.2	21.13	30.93	69.16	115.81	56000	53000

3 Description of the bioclimatic technologies

The following are the main characteristics of the bioclimatic technologies proposed for the NE wing in order to integrate the HVAC system with energy savings measures. Results of the thermal analysis can be used for the SW wing as well. However, specific indications are given in Part III.

3.1 Solar control through shading

The solar control efficacy of a shading device or obstruction acting on a glazed building facade depends on the amount of hours at which the facade is not sunlit (*shading index*) in any given day of the year, particularly during the hottest months. This is related to the obstruction size and projection, the facade orientation, and the geometry of the shading device.

The shading index for a given point on a facade or at ground level, can be evaluated by drawing a shading mask ([3]) of the obstructions at that point and overlapping to it the sun chart of the location, as it was done for the NE wing of the Consalud's building.

3.1.1 *Shading on facades*

The above mentioned overhanging *pergola* shades all facades of the NE wing, while the SW wing and the out-jetting stairs shade the South facade. The shading index for facades North and South was evaluated at the points shown in Drawing 1A (horizontal position) and 1B (vertical position). The relevant elaborated shading masks are represented in Drawing 1C.

As drawing 1C shows, all four points (corresponding, horizontally, to the middle of facade and, vertically, to the middle of each floor – see Drawing 1B) of the North facade are shaded all day during May, June, and July. During the other months, the shading index is progressively decreasing as the winter solstice approaches (with prevailing morning sunlight due to orientation), but increases with height at any given month.

On the South facade, the only unshaded points are the ones on the East part (unobstructed by the SW wing) during the last hours of the day, from April to August. However, the sunlit period of three hours (from 16 to sunset) at the first floor is decreasing down to almost zero at the upper floor.

3.1.2 *Slat configuration of the overhanging pergola*

The geometry of the slats constituting the overhanging *pergola* needs to have the following characteristics in order to avoid that direct solar beams reach the facades (see Drawing 1D):

Slat orientation angle (perpendicular to the slat plane) higher than 90° and less than 180°, measured clockwise from the horizontal position (for the South facade looking at East, and so forth going around the building counter-clockwise).

Tilt angle (from the horizontal plane) higher than zero and less than 90°.

Distance (*D*) between bottom edge of a slat and upper edge of the next one equal or less than zero (positive direction away from the facade).

([3]) Shading masks and solar path diagrams (sun charts) are described in several energy conscious building design handbooks such as: *The Energy Design Handbook*, edited by Donald Watson, EAIA, The American Institute of Architects Press, New York, 1993; Lechner, N., *Heating, Cooling, Lighting – Design Method for Architects*, John Wiley & Sons, New York, 1991.

The distance *D* is related to the cross sectional length (*L*) of the slats and to the thickness of the overhang (*s*) by the following equations (see Drawing 1D):

$$L = \sqrt{s^2\left[1+4\left(\frac{\cos\varepsilon_{max}}{\sin\varepsilon_{max}}\right)^2\right]}$$

$$\varepsilon_{min} = \arccos\left(\frac{s}{L}\right)$$

$$D = \frac{1}{2}L\cos\varepsilon_{min}$$

Where:

L	=	cross sectional length of a slat
s	=	thickness of the overhang
ε_{max}	=	tilt angle of the plane passing through the upper edge of a slat and the bottom edge of the next one (maximum altitude angle of a sun ray passing through the overhang)
ε_{min}	=	tilt angle of a slat (minimum altitude angle of a sun ray passing through the overhang on a plane perpendicular to the facade)
D	=	distance between upper edge of a slat and the bottom edge of the next one

3.2 Glazing type alternatives

Significant energy savings can be achieved by a proper selection of glazing type, particularly, when large transparent surfaces are foreseen as in the Consalud's building NE wing.

The basis configuration (see § 6.1) includes windows with clear double-glass, which have a low *U-value* (3 W/m^2 K), but a high *solar gain factor* ([4]). The thermal characteristics of such a glazing type (*solar transmittance,* τ_s = 0.74, *solar absorptance,* α_s = 0.12, *solar gain factor, SGF* = 0.78) allow for a significant part of solar energy to enter the building. These high solar gains worsen the office space indoor climate conditions as well as the annual thermal loads which are due mainly to cooling needs (see Table 11).

To reduce such solar gains, the following glazing type alternatives were considered:

Clear single glass, which increases thermal losses both in winter and in summer (*U-value* = 5.5 W/m^{2}K, τ_s = 0.78, α_s = 0.15, *SGF* = 0.82).

Double pane window with clear inner glass and absorbing outer glass (τ_s = 0.44, α_s = 0.44, *SGF* = 0.51).

Double pane window with clear inner glass and reflecting outer glass ((τ_s = 0.29, α_s = 0.58, *SGF* = 0.42).

The above-indicated characteristics are standard for each glazing type (clear, absorbing, reflecting). Even lower solar gain factors can be reached using darker absorbing or reflective glass, but low daylight penetration and exterior visual disturbance can be serious backside effects.

([4]) The *solar gain factor* is defined as the ratio of solar transmitted energy through a window to the solar energy incident on the external window plane.

3.3 Thermal control and ventilation through the structural system

3.3.1 *Pillar-ducts*

The designers' choice of combining vertical bearing function and airflow transportation in one building element, a *steel pillar-duct*, is rational and efficient, as long as all relevant joint thermal and structural stress problems are solved.

Based on the maximum airflow rates requirement for ventilation cooling (see § 6.2.3 and 6.2.4), the pillar-duct constant inner cross section is 0.25 m^2.

Pillar-ducts have to be thermally and acoustically insulated. As an optimal solution, a double insulation layer can be applied: an inner mineral- or rock wool matte of not less than 5 cm thickness; an outer at least 2 cm thick gypsum board panel. A protective weatherproof additional layer needs to be foreseen, if a side is externally exposed. A single externally protected panel of high-density polystyrene not less than 6 cm thick, can be foreseen as an alternative simpler solution, but less efficient for acoustical insulation.

Joints between steel pillar-ducts and floor slabs need to be designed properly, e.g., inserting resilient material, in order to avoid risks of sound structural transmission.

3.3.2 *Ventilation of floor slabs*

Building thermal mass plays an important role in attenuating both thermal loads and temperature swings generated within a building. Heat absorbed by a massive structure during the day, can be dissipated by ventilating its exposed surface at night. This ventilation can be natural – wind driven or generated by stack effect – or mechanical.

Floor slabs represent the only thermal mass that can be used as a cooling sink in the NE wing as long as no counter-ceilings are applied. It is suggested that night ventilation of the 15-cm thick floor slabs be done mechanically using the same operational scheme characterising daily ventilation (see § 4.4.4 and 4.4.5). This will mean flushing the slab surface underneath the elevated flooring instead of flushing the ceiling. However, the lower specific cooling efficiency due to this scheme is compensated by an overall better performance of the ventilation system.

3.4 HVAC System

It is proposed a HVAC all-air system using bioclimatic techniques both for heating (solar collectors on roof) and cooling (ventilation with outdoor air and through buried pipes). Description of the system and relevant subsystems as well as its operation schemes is outlined in the following sections.

3.4.1 *HVAC System Description*

The air distribution system is modular. The air volume between two subsequent cross sections along the pillar-ducts is the basis module.

As a first hypothesis to be checked and detailed during the design development, an air-handling unit (AHU.) located at the 2nd underground floor of the NE wing can serve three modules (see Drawings 2 and 4B). AHUs have to be connected to a heating furnace and a chiller through a hot and cold water pipe network. Heating furnace and chiller can be located in the equipment room at the 2nd underground floor of the SW wing.

The proposed HVAC system comprises the following sub-systems and relevant components.

Outdoor air connection (Drawing 5A)

- Solar collectors working as air inlet (winter/day and, possibly, summer/night) or outlet (summer/day).
- Ducts located underneath the solar collectors' plate working as air inlet (summer/day) or outlet (winter/day and, possibly, summer/night).

Vertical air distribution subsystem ([5])

- Air supply and exhaust fans – located on the roof at the base of the solar collectors plate - with acoustical dampers, respectively, downstream and upstream.
- Four-ways flow control box – located downstream the fans – with partial air re-circulation mode when no cooling loads are given (Drawings 5A, 5B).
- Air supply (central) and return (North side) pillar-ducts with net internal cross section of 0.25 m^2; horizontal ductwork connecting them to the flow control box, at the top end, and to the AHUs, at the bottom one (Drawing 4A).
- Room air supply pillar-ducts of 0.25-m^2 net cross section and placed on the South wall (Drawing 4A).
- Water tanks including an overall volume of approximately 15-m^3 and located at the 2nd underground floor (South side) for daily storage of the solar energy collected on roof. As an indication, the number of tanks can be one for each AHU connected to the horizontal duct linking the central air supply pillar-duct to the AHU by an air-water heat exchanger equipped with a by-pass system.
- Air Handling Units for air filtering, cooling, de-humidification, pre- and post-heating with humidification, located at the 2nd underground floor (South side) and in number that will be defined by the HVAC design development; as an indication, an AHU can serve an air volume of three modules and needs a minimum room space of 4×6.25×2.7h (m) (Drawing 4B).

Horizontal air distribution subsystem (Drawing 2, 3A, 3B, 4A) ([6])

Supply:

- Horizontal main air distribution duct of 0.25 m^2 net cross section linked to the above air supply pillar-ducts and located underneath the elevated floor along the South wall. The continuity of this duct along the whole building southern facade allows for a flexible subdivision of the room air distribution ductwork in relation to possible variation of the office room layout.
- Room air supply ducts, one for each module at each floor, hung at the ceiling along the cross section of the building and linked, through the floor slab, to the above-described horizontal main air distribution duct.
- Air diffusion vents placed on the room air supply ducts with operable slats so that air can be distributed where needed.

Exhaust:

- Air outlet grids, one for each module at each floor, placed on the elevated floor along the cross section of the building adjacent to the pillar-ducts on the west side of each module and connecting the room air volume to the *plenum* underneath the elevated floor. They can be placed on a different position or even divided as long as the air room circulation is properly maintained, i.e., not on a vertical alignment to the ceiling air room supply ducts.
- Room return air horizontal ducts of indicative 0.25-m^2 net cross section located underneath the elevated floor to extract air through the plenum. They are placed along the cross section of each floor (opposite to the outlet grid at the eastern side of each module) and connected to the air exhaust pillar-ducts on the northern wall.

([5]) Except for the pillar-ducts, the exact configuration of this subsystem will be defined by the HVAC system design development.

([6]) See note ([5]).

- Return air pillar-ducts of 0.25-m^2 net cross section placed along the northern wall and connecting the return air horizontal ducts to the roof flow control boxes.

Buried pipes subsystem

- Parallel PVC ducts grounded at 2-m depth and placed perpendicularly to the South wall at 0.5-m distance each other. Each duct is constituted of two equal tracts running on a vertical plane with opposite flow directions (at 1.5-m distance) and, possibly, linked by an elbow-shaped joint (Drawing 2). Length, diameter, and number of buried pipes depend on the energy savings, which are wanted to achieve compatibly with site construction constraints.
- Two by-pass boxes intercepting the buried pipes, one at the top (supply air) and the other at the bottom (return air) of the wall, to reach, respectively, a central air supply pillar-duct and a AHU. The net working section of each box needs to be such that all incoming buried pipes are connected (Drawing 4B).

3.4.2 *HVAC System Operation Schemes*

A basic ventilation operation scheme of the proposed HVAC system is applied when air thermo-hygrometric characteristics are neutral, i.e., within the comfort range. In this case, the minimum fresh air change per hour (ACH) required for indoor air quality (30 m^3/person corresponding to 0.6 ACH on average) is satisfied. Outdoor air captured by the ducts on roof is transported through the central pillar-ducts directly to the AHUs for filtering and, possibly, moisture control. From there, air is moved through the southern pillar-ducts to the ceiling room supply ducts.

Different operation schemes will be required when thermo-hygrometric characteristics of air are not neutral, i.e., out of the comfort range. Comfort conditions imply air temperature and humidity values ranging, respectively, from ~20 to ~26 °C and ~40 to ~60 %. In addition, surface internal temperatures do not have to be too different from the air temperature as it should be achieved in the Consalud buildings following the indications given for envelope and horizontal structure.

More precise indications on the comfort conditions can be drawn from parametrical procedures such as Fanger's PMV (Predicted Mean Vote)([7]). An adequate value of this parameter should be achieved in every working hour and day of the year by a proper schedule of the airflow control and handling system.

Two main HVAC comfort operation schemes can be foreseen and described as follows.

Heating

If indoor air temperature is lower than the minimum comfort air temperature, the HVAC system operates in heating mode. Air entering the solar collectors on roof is moved to the AHUs at a variable airflow rate depending on room microclimate conditions. Maximum airflow rate is 3 ACH with re-circulation – when air temperature downstream the room air ventilation system is higher than external air temperature – except for the quote necessary for indoor air quality control.

Airflow control through the by-pass system intercepting each water storage tank along the way from a central supply pillar duct and an AHU depends on the room supply air temperature (t_{rs}) as well as the air temperature downstream solar collectors (t_{sc}) and the water tank temperature (t_{wt}).

The following flow control modes are possible:

$t_{sc} < t_{rs}$ and $t_{wt} > t_{sc}$ air moves through the switched-on heat exchanger whereby is pre-heated before reaching the AHU

$t_{sc} < t_{rs}$ and $t_{sc} > t_{wt}$ air moved through the water tank by-pass or the switched-off heat exchanger

([7]) Fanger, P.O., *Thermal Comfort*, Mc Graw Hill, New York, 1970.

$t_{sc} > t_{rs}$ and $t_{sc} > t_{wt}$ air moves through the switched-on heat exchanger to charge the storage water tank before reaching the AHU

$t_{sc} > t_{rs}$ and $t_{sc} < t_{wt}$ air moves through the water tank by-pass or the switched-off heat exchanger

Cooling

If indoor air temperature is higher than the maximum comfort air temperature, the HVAC system operates in cooling mode. Air entering the ducts or collectors (possibly, at night) on roof is moved to the AHUs at a variable airflow rate depending on room microclimate conditions. Maximum airflow rate is 3 ACH with re-circulation – when air temperature downstream the room air ventilation system is lower than external air temperature – except for the quote necessary for indoor air quality control.

Airflow control through the four-ways box on roof and through the by-pass system intercepting each module set of buried pipes depends on external air temperature (t_e) as well as duct air temperature downstream the solar collectors (t_{sc}) and the buried pipes (t_{bp}).

The following flow control modes are possible:

$t_{sc} < t_e$ and $t_{sc} < t_{bp}$ (night) air enters the solar collectors and is moved directly to the AHUs

$t_{bp} < t_e$ and $t_{bp} < t_{sc}$ air enters the ducts on roof and is moved to the buried pipes before reaching the AHUs

$t_e < t_{sc}$ and $t_e < t_{bp}$ air enters the ducts on roof and is moved directly to the AHUs

4 Thermal analysis

A thermal analysis was performed for the NE wing using the above mentioned simulation code QUICKII. Input data are:

- zone orientation and dimensions;
- occupants and internal loads;
- operational parameters such as natural and mechanical ventilation rates as well as plant working period and set-point values for air temperature and humidity.

Thermal simulation was first carried out on a basis configuration. Afterwards, input data were added, or changed, in relation to the various bioclimatic technologies proposed in order to obtain the relevant energy savings.

4.1 Basis configuration

4.1.1 *Zone data*

The NE wing was divided in six zones: one office space for each floor, including both open and subdivided spaces, the out-jetting south stairs well, and the toilet rooms at each floor.

The zone characteristics required by the code are shown in Table 9, except for the toilet rooms, which should be air conditioned by means of a simple extraction strategy. Operational data, i.e., occupancy level, minimum required air change rate, and internal loads were differentiated according to three week day periods: entry/exit hour, working hours, and lunch break hour.

The daily occupancy level was given by the design team and divided by two in the lunch break. The entry/exit hour occupancy level was differentiated from the one at working hours only for the stairs zone. The minimum required air change rate was defined on the basis of 30 ACH/person.

Beside the occupancy loads, sensitive, convective, and radiative loads due to appliances, were considered taking one workstation (PC + printer) per employee into account plus two photocopier at each floor. Furthermore, radiant internal loads were calculated on the basis of a minimum luminance requirement on horizontal plane ranging from 200 (passage areas) to 300 (working area) lumen/m^2 with an utilisation factor of 50% and a lamp efficiency of 70 lumen/W.

The zones at third and fourth floor have the same occupancy, ventilation, and internal gain data of the zones at first and second floor, in spite of a larger area. This is due to the characteristics of the upper zones, which are less occupancy intensive being foreseen for directional single office rooms.

Table 9 – Zone characteristics for thermal analysis

PARAMETERS		ZONE			
		1st floor	2nd floor	3rd / 4th floor	South stairs well
Reference azimuth		21°	21°	21°	21°
Area (m^2)	roof	1314	1314	1681	90
	base floor	1314	1314	1681	48
	base floor (void)				42
Volume (m^3)		4349	4349	5566	360
Occupancy (n. of persons)	entry/exit hour	125	125	125	100
	working hours	125	125	125	30
	lunch break	63	63	63	50
Mechanical ventilation (ACH)	entry/exit hour	0,5	0,5	0,5	8,5
	working hours	0,5	0,5	0,5	2,5
	lunch break	0,3	0,3	0,3	4,3
Sensible internal loads (kW):					
radiant	entry/exit hour	13	13	13	1
	working hours	11	11	11	1
	lunch break	7	7	7	1
convective	entry/exit hour	54	54	54	0
	working hours	54	54	54	0
	lunch break	36	36	36	0
total	entry/exit hour	67	67	67	1
	working hours	65	65	65	1
	lunch break	43	43	43	1
total per unit area (W/m^2)	entry/exit hour	51	51	40	11
	working hours	50	50	39	11
	lunch break	33	33	26	11

4.1.2 *Building components data*

Building components' characteristics were defined for thermal simulation as a result of a long interactive process involving the consultants and the design team and aimed to find optimal choices responding to energy saving as well as technological requirements.

The latest choices used for final simulation are shown in Table 10. Dimensions indicated there are not meant to be design constraints but simply reference values for thermal simulation.

Table 10 – Input values for building components

BUILDING COMPONENT	AREA (m^2)					LAYERS (*) (mm)	
	1st floor	2nd floor	3rd floor	4th floor	South stairs well		
External west wall	19.02	22.17				10 plaster 50 insulation layer 150 concrete poured 10 plaster	
External windows:						Glass:	
north glass	208.75	161.45	196.05	196.05		4 glass 9 airspace 4 glass	
east glass	42.36	27.85	25.24	25.24			
south glass	164.01	126.86	155.69	155.69			
west glass			28.50	28.50			
south-east glass					105.00		
south-west glass					105.00	Frame:	
north frame	36.14	28.49	28.49	28.49		2 Aluminium 56 airspace 2 Aluminium	
east frame	6.35	4.91	4.91	4.91			
south frame	28.93	22.37	22.37	22.37			
west frame			4.14	4.14			
south-east frame					16.00		
south-west frame					16.00		
Parapet:							
north parapet		55.65	133.37	133.37		2 Aluminium 96 rigid grid and insulation layer 2 Aluminium	
east parapet		22.40	14.84	14.84			
south parapet		43.72	108.80	108.80			
west parapet			16.76	16.76			
External structural wall: north pillar-duct south pillar-duct	43.35 41.77	50.30 48.46	51.14 50.30	51.14 50.30		2 Aluminium 50 insulation layer 20 structural steel 500 inner duct airspace 20 structural steel	
Entrance door	9.45	6.30	6.30	6.30		60 wood pine	
Internal door	31.28	31.28	31.28	31.28		5 wood-ply 40 airspace 5 wood-ply	
Internal structural wall	187.05	191.31	191.31	191.31		10 plaster 180 concrete poured 10 plaster	
Internal wall	28.40	28.40	28.40	28.40		100 gypsum plaster board	
Low partitions	779.12	779.12	779.12	779.12		5 carpet 70 wood-ply 5 carpet	
Floor	1314.00	1314.00	1681.00	1681.00	48.00	2 carpet 28 hardboard 350 airspace 200 concrete poured (1st floor)	2 carpet 28 hardboard 350 airspace 150 concrete poured (2nd ,3rd and 4th)
Roof	1314.00	1314.00	1681.00	1681.00	90.00	20 flooring (tiles) 3 waterproof layer 50 insulation layer 0.5 water vapour barrier 350 concrete poured	

(*) Layers are listed from exterior to interior for vertical components, and from top to bottom for horizontal components.

4.1.3 *Reference Cooling and Heating Energy*

The thermal simulation results for the basis configuration, i.e., the reference monthly and annual cooling and heating energy are shown in Table 11.

Table 11 - Annual energy: basis configuration (kWh)

Month	Cooling energy		
	Sensible	Latent	Total
Jan	99000	5098	104098
Feb	93900	4689	98589
Mar	102800	4652	107452
Apr	71800	3142	74942
May	58700	1922	60622
Jun	46000	1285	47285
Jul	52800	1001	53801
Ago	50300	1419	51719
Sep	56600	1952	58552
Oct	79400	2668	82068
Nov	79500	3440	82940
Dec	89200	4093	93293
Total	**880000**	**35361**	**915361**

Month	Heating energy		
	Sensible	Latent	Total
Jan	570	50	620
Feb	970	42	1012
Mar	2380	64	2444
Apr	5840	126	5966
May	9300	222	9522
Jun	12670	314	12984
Jul	13510	452	13825
Ago	12360	315	12555
Sep	6910	195	7077
Oct	3920	167	4019
Nov	2340	99	2422
Dec	1230	82	1312
Total	**72000**	**2128**	**73758**

As Table 11 shows, March and July are the month with the highest, respectively, cooling and heating energy. However, annual heating energy is less than 10% of the annual cooling energy.

4.2 Energy savings for the various technologies

Energy savings achievable applying the above described technologies are indicated below with reference to the monthly and annual energy foreseen by simulation for the basis configuration and shown in Table 11 (REACE = reference estimated annual cooling energy, REAHE = reference estimated annual heating energy).

4.2.1 *Solar control through the overhangs*

Monthly and annual energy for the basis configuration with added effect of the overhanging *pergola* are indicated in Table 12.

As table 12 compared to table 11 shows, the installation of a *pergola* induces savings for 110 MWh (13% of REACE) while increases REAHE by 80% (58 MWh). The overall yearly balance still implies energy savings (– 52 MWh). In addition, the heating energy increment can be covered by free-cost solar energy (see § 5.2.5).

Table 12 - Annual energy: basis configuration with overhangs (kWh)

Month	Cooling energy		
	Sensible	Latent	Total
Jan	82500	5046	87546
Feb	77800	4640	82440
Mar	89300	4604	93904
Apr	63700	3107	66807
May	53000	1896	54896
Jun	45700	1352	47052
Jul	47800	983	48783
Ago	46700	1397	48097
Sep	55800	2119	57919
Oct	67000	2635	69635
Nov	65500	3401	68901
Dec	75200	4048	79248
Total	**770000**	**35228**	**805228**

Month	Heating energy		
	Sensible	Latent	Total
Jan	1100	50	1150
Feb	1800	42	1842
Mar	4180	64	4244
Apr	9670	126	9796
May	16130	222	16352
Jun	23290	314	23604
Jul	24600	452	25052
Ago	21660	315	21975
Sep	13460	195	13655
Oct	8000	167	8167
Nov	4030	99	4129
Dec	2080	82	2162
Total	**130000**	**2128**	**132128**

4.2.2 *Effect of various glazing types*

The monthly and annual estimated energy related to the basis configuration where double clear glass was substituted with single glass, double glass with absorbing external pane, and double glass with reflective external pane – as described in § 4.2 – are shown in Table 13a, 13b, and 13c, respectively.

Table 13a - Annual energy: basis configuration with single glass (kWh)

Month	Cooling energy		
	Sensible	Latent	Total
Jan	101900	5034	106934
Feb	94900	4632	99532
Mar	102700	4593	107293
Apr	66400	3096	69496
May	48700	2273	50973
Jun	35100	1336	36436
Jul	41700	1070	42770
Ago	39200	1388	40588
Sep	55000	2109	57109
Oct	73800	2625	76425
Nov	77600	3394	80994
Dec	89200	4039	93239
Total	**826200**	**35589**	**861789**

Month	Heating energy		
	Sensible	Latent	Total
Jan	910	50	960
Feb	1390	42	1432
Mar	3110	64	3174
Apr	7100	126	7226
May	11090	222	11312
Jun	15770	286	16056
Jul	16560	455	17015
Ago	14650	316	14966
Sep	8390	195	8585
Oct	4900	167	5067
Nov	2960	99	3059
Dec	1650	82	1732
Total	**88480**	**2104**	**90584**

Table 13b - Annual energy: basis configuration with absorbing double glass (kWh)

Month	Cooling energy		
	Sensible	Latent	Total
Jan	93600	5046	98646
Feb	86200	4639	90839
Mar	91100	4602	95702
Apr	64100	3103	67203
May	50300	1894	52194
Jun	41400	1350	42750
Jul	46000	980	46980
Ago	45000	1395	46395
Sep	54600	2116	56716
Oct	70700	2635	73335
Nov	74400	3401	77801
Dec	85600	4048	89648
Total	**803000**	**35209**	**838209**

Month	Heating energy		
	Sensible	Latent	Total
Jan	660	50	710
Feb	1080	42	1122
Mar	2580	64	2644
Apr	6050	126	6176
May	10420	222	10642
Jun	14280	314	14594
Jul	15130	453	15583
Ago	13220	315	13535
Sep	7860	195	8055
Oct	4360	167	4527
Nov	2530	99	2629
Dec	1310	82	1392
Total	**79480**	**2129**	**81609**

Table 13c - Annual energy: basis configuration with reflecting double glass (kWh)

Month	Cooling energy		
	Sensible	Latent	Total
Jan	90300	5045	95345
Feb	81700	4638	86338
Mar	85600	4601	90201
Apr	59400	3103	62503
May	49200	1892	51092
Jun	39700	1349	41049
Jul	41900	980	42880
Ago	41900	1395	43295
Sep	51300	2116	53416
Oct	65100	2633	67733
Nov	70800	3401	74201
Dec	83100	4048	87148
Total	**760000**	**35201**	**795201**

Month	Heating energy		
	Sensible	Latent	Total
Jan	700	50	750
Feb	1120	42	1162
Mar	2650	64	2714
Apr	6180	126	6306
May	10330	222	10552
Jun	14910	314	15224
Jul	15750	453	16203
Ago	13120	315	13435
Sep	8320	195	8515
Oct	4750	167	4917
Nov	2630	99	2729
Dec	1340	82	1422
Total	**81800**	**2129**	**83929**

The annual energy savings for the simulated glazing types can be drawn comparing data in Tables 13 to the ones in Table 11. They are the following.

Single glass: 17 MWh added for heating (24% of REAHE) Vs 53.8 MWh less for cooling (6% of REACE);

Absorbing double glass: +8 MWh (11% of REAHE) Vs –77 MWh (9% of REACE);

Reflective double glass: +10 MWh (14% of REAHE) Vs –120 MWh (14% of REACE).

The balanced savings are: –36.8 MWh (single glass), –69 MWh (absorbing double glass), and –110 MWh (reflective double glass). The latest is the most energy saving configuration. However,

the adoption of double glass with an absorbing external pane is suggested due to the negative effect of reflective glazing on daylighting and external microclimate.

4.2.3 *Night ventilation*

Mechanical instead of natural night ventilation of spaces and thermal mass was chosen due to various reasons. Wind, the main driving force for natural ventilation at night, has a stochastic behaviour and a relative low speed. Using the same mechanical ventilation system at night and during office hours has a higher operational efficiency. Furthermore, night natural ventilation requires top ceiling opening windows considered, by the architectural designers, too costly and complex to be operated.

Thermal simulation for the basis configuration with added mechanical night ventilation was carried out at two ACH: 0.5 and 3.

From the simulation results shown in Table 14a and 14b, compared to the reference data (Table 11), sensible energy savings obtainable by mechanical night ventilation are the following.

0.5 ACH: +1.4 MWh (2 % of REAHE), –44 MWh (5 % of REACE); balanced savings are –42.6 MWh.

3 ACH: +8.4 MWh (13 % of REAHE), –176 MWh (20 % of REACE); balanced savings are –167.6 MWh.

The slight augmented sensible heating load, increasing with ACH, is due to the effect of cool air ventilation at the earliest hours of the day just before 8 and can be easily avoided by a variable flow rate control. According to the simulation results, cooling effectiveness of mechanical night ventilation increases with air change rate. Nevertheless, the actual operational rates have to be set in relation to the specific variable indoor climate conditions, considering also a balance between thermal potential energy savings and the relevant increase in electricity consumption for fans. This is another reason for choosing a variable air change rate control system.

Table 14a - Annual energy: basis configuration with night ventilation at 0.5 ACH (kWh)

Month	**Cooling energy**		
	Sensible	Latent	Total
Jan	98100	5021	103121
Feb	91900	4656	96556
Mar	101100	4495	105595
Apr	68900	2886	71786
May	53400	1802	55202
Jun	41700	1301	43001
Jul	47500	955	48455
Ago	45900	1341	47241
Sep	49100	1983	51083
Oct	74300	2423	76723
Nov	76100	3172	79272
Dec	88000	3860	91860
Total	**836000**	**33895**	**869895**

Month	**Heating energy**		
	Sensible	Latent	Total
Jan	650	50	700
Feb	1040	42	1082
Mar	2500	64	2564
Apr	5950	229	6179
May	9350	630	9980
Jun	13100	842	13942
Jul	13920	1075	14995
Ago	12080	841	12921
Sep	7110	522	7632
Oct	3960	335	4295
Nov	2420	99	2519
Dec	1310	82	1392
Total	**73390**	**4811**	**78201**

Table 14b - Annual energy: basis configuration with night ventilation at 3 ACH (kWh)

Month	Cooling energy		
	Sensible	Latent	Total
Jan	94600	5010	99610
Feb	89200	4636	93836
Mar	94400	4474	98874
Apr	57300	2873	60173
May	36100	1779	37879
Jun	24200	1283	25483
Jul	28500	940	29440
Ago	27900	1231	29131
Sep	40400	1965	42365
Oct	61400	2411	63811
Nov	66900	3159	70059
Dec	83100	3858	86958
Total	**704000**	**33619**	**737619**

Month	Heating energy		
	Sensible	Latent	Total
Jan	830	50	880
Feb	1160	42	1202
Mar	2600	64	2664
Apr	5720	272	5992
May	9760	673	10433
Jun	15030	888	15918
Jul	15830	1123	16953
Ago	13740	887	14627
Sep	7700	538	8238
Oct	4080	351	4431
Nov	2550	99	2649
Dec	1400	82	1482
Total	**80400**	**5069**	**85469**

4.2.4 *Ventilation through buried pipes*

The energy saving effectiveness of a HVAC-integrated ventilation system such as the one here proposed, which uses buried pipes to pre-cool air before it enters the air handling units, depends on the air temperature at the outlet of the grounded ducts. Various pipes configurations - in terms of material, number, length, depth, radius, and air velocity – were simulated using the code SUMMER, Version 2, module TECHNIQUES ([8]), in order to obtain outlet monthly air temperatures for the climate of Santiago. PVC 70 m long buried pipes located at 2-m depth, with diameter of 20 cm and air velocity of 10 m/s, obtained the best performance. Inlet (outdoor) and outlet air temperature, at every month, for a buried pipe in the configuration described above, and two diameters (20 and 40 cm) are shown in tables 15 and figures 4.

Airflow rates are 1130 m^3/s for the pipe with 20 cm diameter and 4520 m^3/s for the one with 40 cm diameter. The net volume of a HVAC module of the NE wing is approximately 1500 m^3 (375 m^3 at each floor). Hence, one 40-cm diameter buried pipe can serve an entire module at 3 ACH, while four 20-cm diameter pipes are needed to supply the same amount of air volume.

([8]) Klitsikas, N., et Al., SUMMER Version 2.0, A tool for Passive Cooling of Buildings, EC DG XVII for Energy – SAVE Programme, CIENE, University of Athens, Athens, 1997.

Table 15 – Inlet and outlet hourly air temperatures for buried pipes at each month

Month: January			
Standard time	Air temperatures [°C]		
	$t_{air,in}$	$t_{air,out\ d=20\ cm}$	$t_{air,out\ d=40\ cm}$
1	15.8	16.9	16.9
2	14.2	16.1	15.7
3	12.8	15.4	14.6
4	11.9	14.8	13.8
5	11.5	14.5	13.4
6	11.9	14.5	13.5
7	13.1	14.9	14.1
8	15.1	15.7	15.4
9	17.7	16.8	17.1
10	20.7	18.1	19.2
11	23.6	19.4	21.3
12	26.2	20.6	23.2
13	28.2	21.6	24.7
14	29.4	22.4	25.8
15	29.8	22.7	26.2
16	29.5	22.7	26.2
17	28.5	22.5	25.7
18	27.1	22	24.9
19	25.6	21.4	23.9
20	23.9	20.7	22.8
21	22.3	20	21.6
22	20.7	19.3	20.5
23	19	18.5	19.3
24	17.4	17.7	18.1
Average	20.7	18.7	19.9

Month: February			
Standard time	Air temperatures [°C]		
	$t_{air,in}$	$t_{air,out\ d=20\ cm}$	$t_{air,out\ d=40\ cm}$
1	17.2	17.5	17.8
2	15.7	16.8	16.7
3	14	16	15.5
4	12.4	15.2	14.3
5	11.3	14.5	13.4
6	10.8	14.1	12.8
7	11.3	14.2	12.9
8	12.9	14.7	13.9
9	15.3	15.7	15.4
10	18.4	17	17.5
11	21.8	18.5	19.8
12	24.9	20	22.1
13	27.4	21.2	24
14	28.9	22	25.3
15	29.4	22.5	25.9
16	29	22.5	25.8
17	27.8	22.1	25.2
18	26.2	21.6	24.2
19	24.5	20.9	23.1
20	23	20.2	22
21	21.7	19.6	21.1
22	20.6	19.1	20.3
23	19.6	18.6	19.5
24	18.5	18.1	18.7
Average	20.1	18.4	19.5

Cont.ed Table 15 – Inlet and outlet hourly air temperatures for buried pipes at each month

Month: March			
Standard time	Air temperatures [°C]		
	$t_{air,in}$	$t_{air,out\ d=20\ cm}$	$t_{air,out\ d=40\ cm}$
1	15.3	16.3	16.1
2	13.8	15.6	15.1
3	12.2	14.8	13.9
4	10.7	14	12.8
5	9.5	13.3	11.8
6	9.1	13	11.3
7	9.6	13	11.4
8	11.1	13.6	12.3
9	13.5	14.5	13.8
10	16.5	15.8	15.8
11	19.8	17.3	18.1
12	22.8	18.7	20.3
13	25.2	19.9	22.2
14	26.7	20.7	23.4
15	27.2	21.1	24
16	26.8	21.2	24
17	25.6	20.8	23.3
18	24.1	20.3	22.4
19	22.5	19.6	21.3
20	21	19	20.3
21	19.7	18.4	19.3
22	18.6	17.8	18.5
23	17.7	17.4	17.8
24	16.6	16.9	17.1
Average	18.2	17.2	17.8

Month: April			
Standard time	Air temperatures [°C]		
	$t_{air,in}$	$t_{air,out\ d=20\ cm}$	$t_{air,out\ d=40\ cm}$
1	14.3	14.9	14.7
2	13.4	14.5	14.1
3	11.9	13.9	13.1
4	10.1	13	11.8
5	8.3	12.1	10.5
6	6.9	11.4	9.4
7	6.3	10.9	8.7
8	6.9	11	8.9
9	8.7	11.6	10
10	11.4	12.8	11.7
11	14.7	14.2	14
12	18	15.7	16.3
13	20.7	17.1	18.4
14	22.4	18	19.8
15	23	18.5	20.5
16	22.5	18.5	20.4
17	21.1	18	19.6
18	19.3	17.3	18.4
19	17.5	16.5	17.2
20	16	15.8	16.1
21	15.1	15.4	15.4
22	14.7	15.1	15
23	14.7	15.1	14.9
24	14.6	15	14.8
Average	14.7	14.8	14.7

Cont.ed Table 15 – Inlet and outlet hourly air temperatures for buried pipes at each month

Month: May			
Standard time	Air temperatures [°C]		
	$t_{air,in}$	$t_{air,out\ d=20\ cm}$	$t_{air,out\ d=40\ cm}$
1	11.2	12.7	11.9
2	10.4	12.3	11.4
3	9.2	11.8	10.6
4	7.8	11.1	9.6
5	6.3	10.4	8.4
6	5.1	9.7	7.5
7	4.7	9.4	7
8	5.2	9.4	7.2
9	6.6	10	8
10	8.8	10.9	9.4
11	11.5	12.1	11.3
12	14.2	13.3	13.2
13	16.4	14.4	14.9
14	17.8	15.2	16.1
15	18.3	15.6	16.6
16	17.9	15.6	16.5
17	16.8	15.3	15.9
18	15.3	14.7	15
19	13.8	14	13.9
20	12.6	13.4	13
21	11.9	13	12.5
22	11.6	12.9	12.2
23	11.5	12.8	12.1
24	11.5	12.8	12
Average	11.5	12.6	11.9

Month: June			
Standard time	Air temperatures [°C]		
	$t_{air,in}$	$t_{air,out\ d=20\ cm}$	$t_{air,out\ d=40\ cm}$
1	8.7	10.8	9.6
2	8	10.5	9.1
3	7	10.1	8.5
4	5.7	9.4	7.6
5	4.3	8.7	6.5
6	3.3	8.2	5.7
7	3	7.9	5.3
8	3.4	7.9	5.4
9	4.6	8.4	6.2
10	6.6	9.2	7.4
11	9	10.3	9.1
12	11.3	11.4	10.8
13	13.3	12.4	12.3
14	14.6	13.1	13.4
15	15	13.4	13.8
16	14.6	13.4	13.7
17	13.6	13.1	13.2
18	12.3	12.6	12.3
19	11	12	11.4
20	9.9	11.5	10.6
21	9.3	11.1	10.1
22	9	10.9	9.8
23	9	10.9	9.8
24	8.9	10.9	9.7
Average	9.0	10.8	9.6

Cont.ed Table 15 – Inlet and outlet hourly air temperatures for buried pipes at each month

Month: July			
Standard time	Air temperatures [°C]		
	$t_{air,in}$	$t_{air,out\ d=20\ cm}$	$t_{air,out\ d=40\ cm}$
1	8.2	10.3	9.1
2	7.5	10	8.7
3	6.5	9.6	8
4	5.2	9	7.1
5	3.8	8.3	6.1
6	2.8	7.7	5.2
7	2.4	7.4	4.8
8	2.9	7.5	4.9
9	4.2	7.9	5.7
10	6.1	8.8	7
11	8.5	9.8	8.6
12	10.9	10.9	10.3
13	12.8	11.9	11.8
14	14.1	12.6	12.9
15	14.5	13	13.4
16	14.2	13	13.3
17	13.2	12.7	12.8
18	11.8	12.1	11.9
19	10.5	11.5	10.9
20	9.5	11	10.2
21	8.8	10.7	9.6
22	8.5	10.5	9.4
23	8.5	10.4	9.3
24	8.5	10.4	9.3
Average	8.5	10.3	9.2

Month: August			
Standard time	Air temperatures [°C]		
	$t_{air,in}$	$t_{air,out\ d=20\ cm}$	$t_{air,out\ d=40\ cm}$
1	9.4	11.1	10.2
2	8.7	10.8	9.7
3	7.6	10.3	9
4	6.1	9.6	7.9
5	4.7	8.9	6.9
6	3.6	8.3	6
7	3.2	7.9	5.5
8	3.6	8	5.7
9	5	8.5	6.4
10	7.2	9.4	7.9
11	9.8	10.6	9.7
12	12.4	11.8	11.6
13	14.5	12.9	13.2
14	15.9	13.6	14.3
15	16.4	14	14.9
16	16	14	14.8
17	14.9	13.7	14.2
18	13.4	13.1	13.2
19	12	12.4	12.2
20	10.8	11.9	11.4
21	10.1	11.5	10.8
22	9.8	11.3	10.5
23	9.8	11.3	10.4
24	9.7	11.2	10.4
Average	9.8	11.1	10.3

Cont.ed Table 15 – Inlet and outlet hourly air temperatures for buried pipes at each month

Month: September			
Standard time	Air temperatures [°C]		
	$t_{air,in}$	$t_{air,out\ d=20\ cm}$	$t_{air,out\ d=40\ cm}$
1	9.7	11.7	10.8
2	8.5	11.2	10
3	7.2	10.5	9
4	6	9.9	8.1
5	5.2	9.4	7.4
6	4.8	9.1	7
7	5.2	9.1	7.1
8	6.4	9.6	7.8
9	8.2	10.3	9
10	10.6	11.4	10.6
11	13.1	12.5	12.4
12	15.5	13.6	14.1
13	17.3	14.6	15.5
14	18.5	15.3	16.5
15	18.9	15.6	17
16	18.5	15.6	16.9
17	17.6	15.3	16.4
18	16.4	14.8	15.6
19	15.2	14.3	14.8
20	14	13.8	14
21	13	13.3	13.3
22	12.2	12.9	12.6
23	11.5	12.6	12.1
24	10.6	12.2	11.5
Average	11.8	12.4	12.1

Month: October			
Standard time	Air temperatures [°C]		
	$t_{air,in}$	$t_{air,out\ d=20\ cm}$	$t_{air,out\ d=40\ cm}$
1	12.1	13.5	13
2	10.8	12.9	12.1
3	9.4	12.2	11.1
4	8.1	11.5	10.1
5	7.1	10.9	9.3
6	6.7	10.6	8.8
7	7.1	10.6	8.9
8	8.4	11.1	9.6
9	10.5	11.9	11
10	13.1	13.1	12.8
11	15.9	14.3	14.7
12	18.5	15.6	16.6
13	20.5	16.6	18.2
14	21.8	17.3	19.3
15	22.3	17.7	19.8
16	21.9	17.7	19.7
17	20.9	17.4	19.2
18	19.6	16.9	18.4
19	18.2	16.3	17.5
20	16.9	15.8	16.5
21	15.8	15.2	15.7
22	14.9	14.8	15.1
23	14.1	14.4	14.5
24	13.1	14	13.8
Average	14.5	14.3	14.4

Cont.ed Table 15 – Inlet and outlet hourly air temperatures for buried pipes at each month

Month: November			
Standard time	Air temperatures [°C]		
	$t_{air,in}$	$t_{air,out\ d=20\ cm}$	$t_{air,out\ d=40\ cm}$
1	12.7	14.5	14
2	11.2	13.7	12.9
3	9.9	13	11.9
4	9	12.5	11.1
5	8.7	12.2	10.7
6	9.1	12.2	10.8
7	10.2	12.6	11.4
8	12.1	13.3	12.6
9	14.5	14.4	14.2
10	17.3	15.6	16.2
11	20	16.8	18.1
12	22.4	18	19.9
13	24.3	19	21.4
14	25.4	19.6	22.3
15	25.8	20	22.8
16	25.5	20	22.8
17	24.6	19.7	22.3
18	23.3	19.3	21.5
19	21.8	18.7	20.5
20	20.3	18	19.5
21	18.8	17.4	18.5
22	17.3	16.7	17.4
23	15.7	16	16.3
24	14.2	15.2	15.1
Average	17.3	16.2	16.8

Month: December			
Standard time	Air temperatures [°C]		
	$t_{air,in}$	$t_{air,out\ d=20\ cm}$	$t_{air,out\ d=40\ cm}$
1	14.7	16	15.9
2	13.1	15.2	14.7
3	11.8	14.5	13.6
4	10.9	14	12.9
5	10.5	13.6	12.4
6	10.9	13.6	12.5
7	12.1	14.1	13.2
8	14.1	14.8	14.4
9	16.6	15.9	16.1
10	19.5	17.2	18.1
11	22.4	18.5	20.2
12	25	19.7	22.1
13	26.9	20.7	23.6
14	28.1	21.4	24.6
15	28.5	21.7	25.1
16	28.2	21.8	25.1
17	27.2	21.5	24.6
18	25.9	21	23.8
19	24.3	20.4	22.7
20	22.7	19.8	21.6
21	21.1	19	20.5
22	19.5	18.3	19.4
23	17.9	17.6	18.2
24	16.3	16.8	17.1
Average	19.5	17.8	18.9

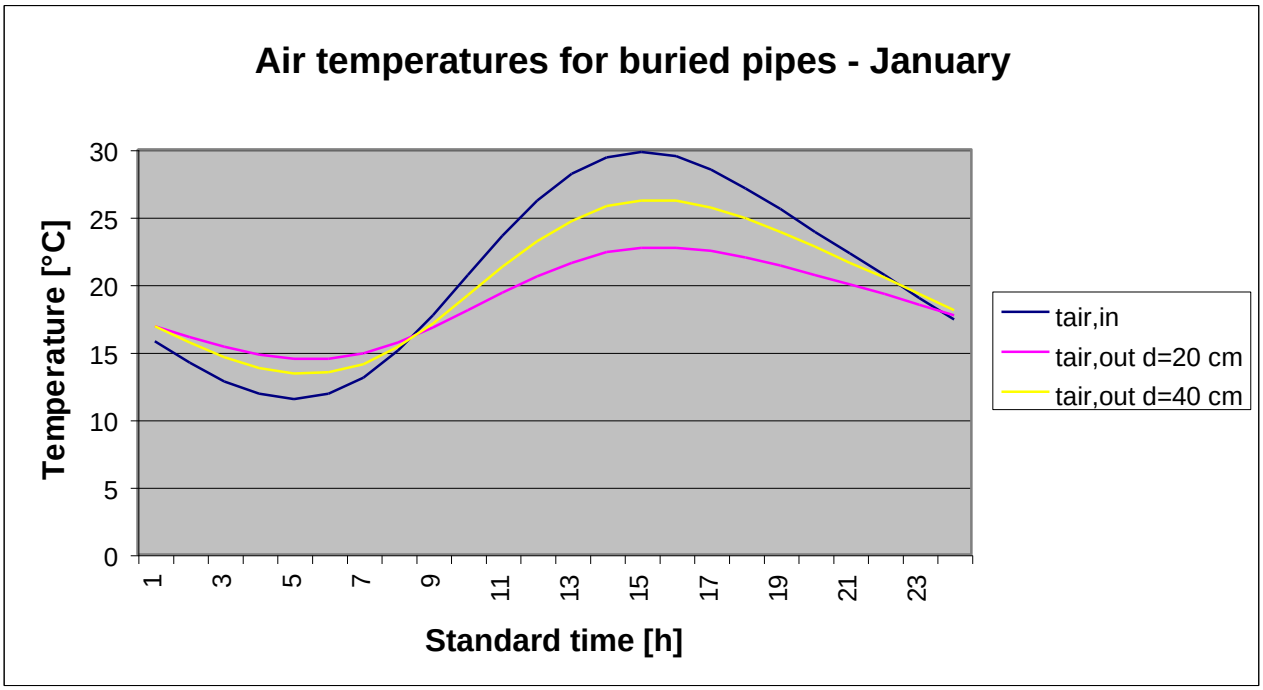

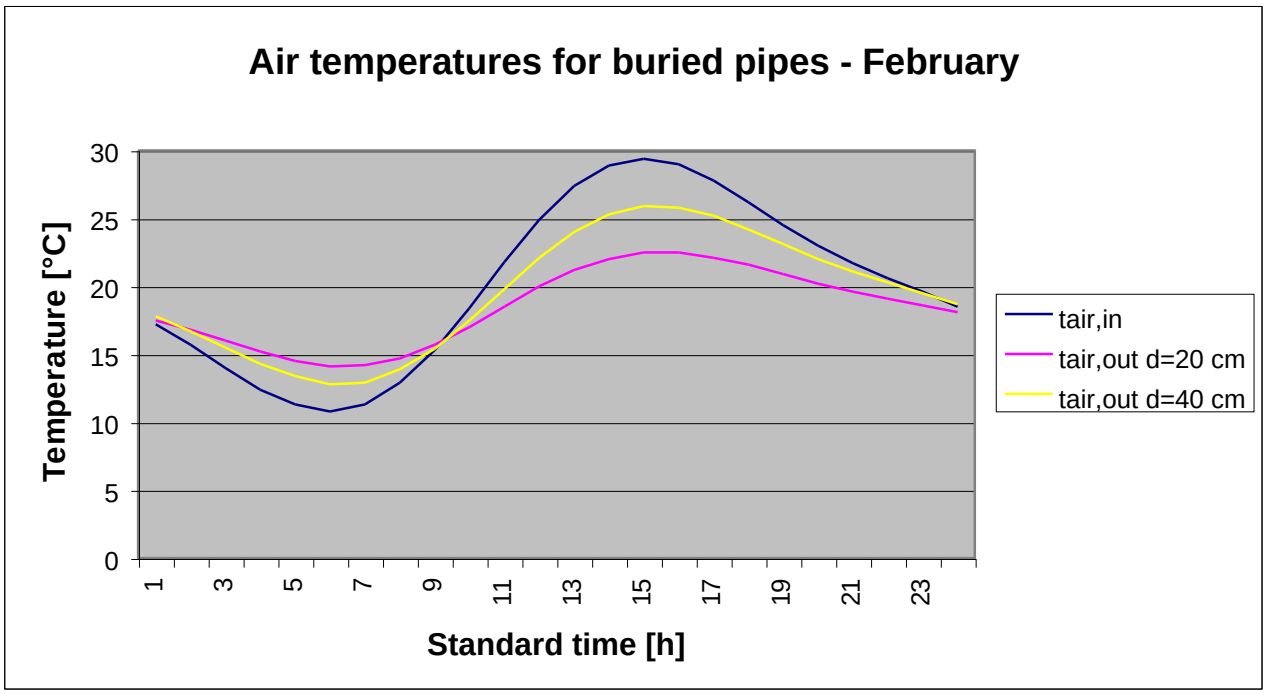

Fig 4 – Inlet and outlet hourly air temperature profiles for buried pipes at each month

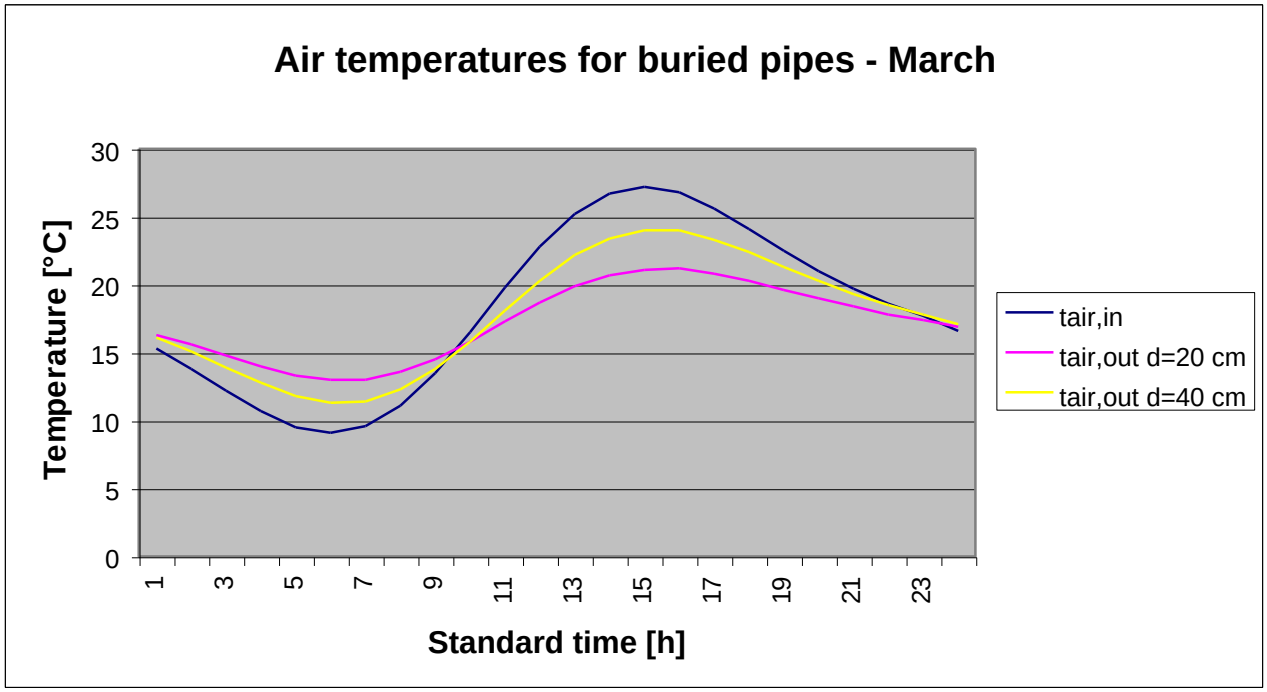

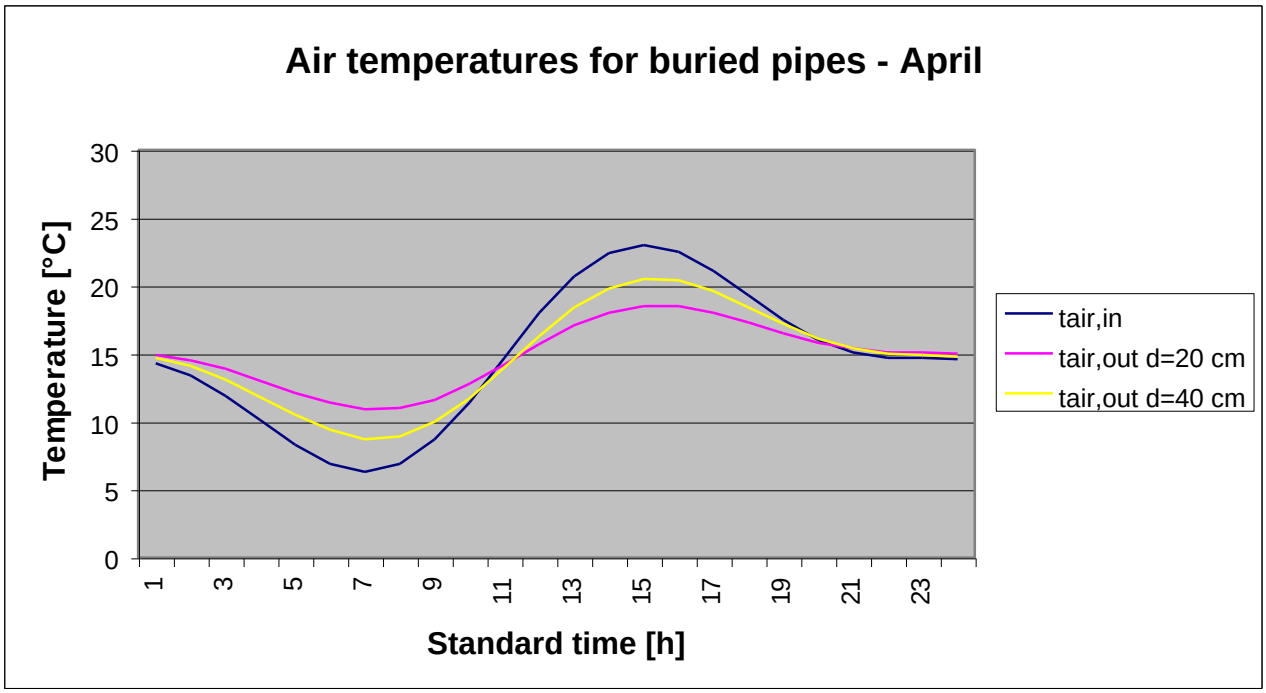

Cont.ed Fig 4 – Inlet and outlet hourly air temperature profiles for buried pipes at each month

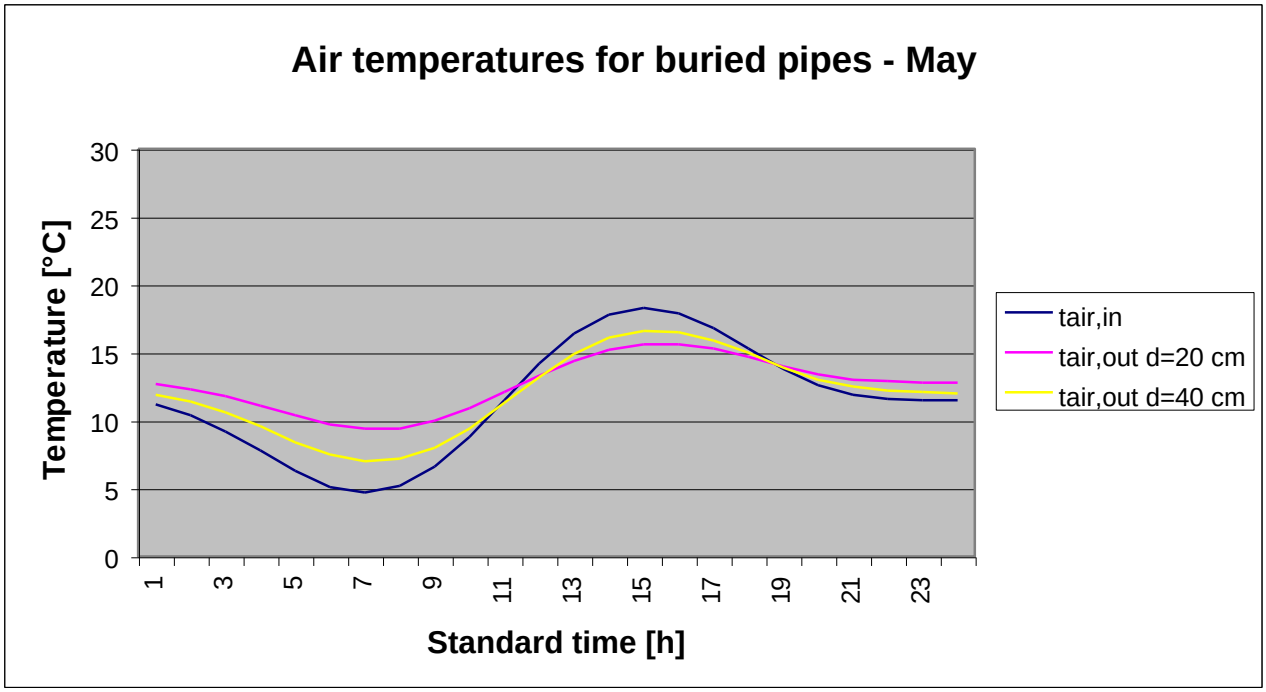

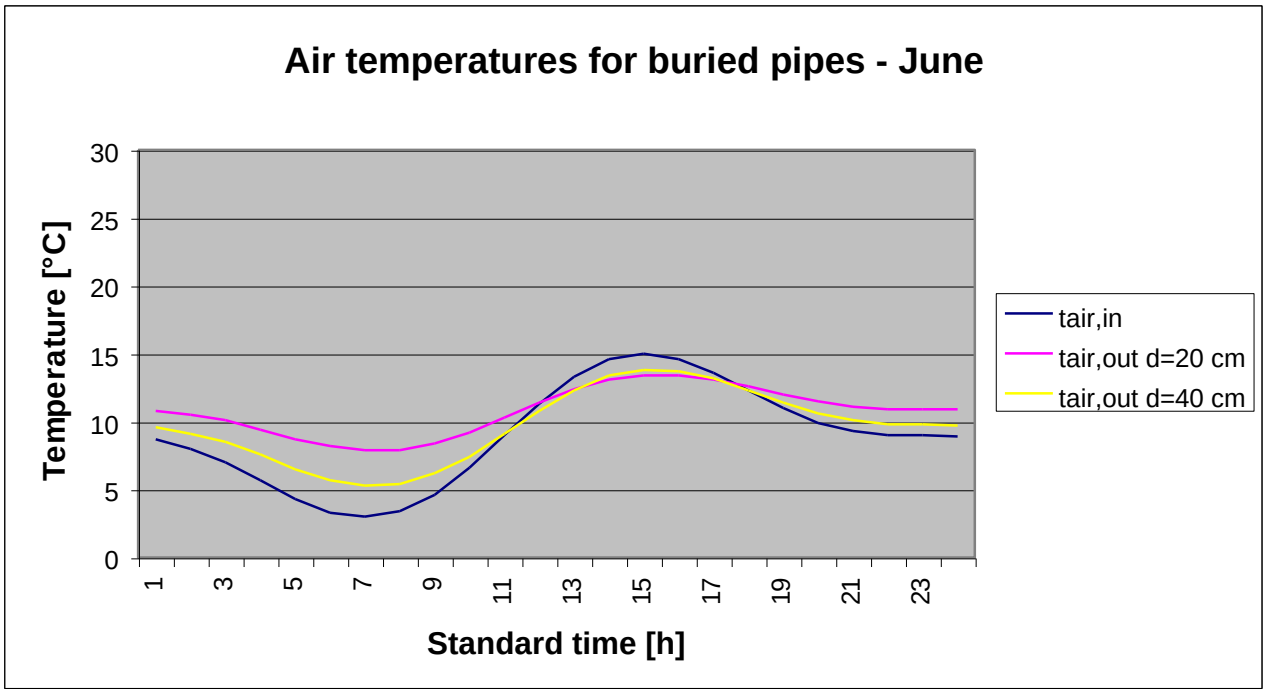

Cont.ed Fig 4 – Inlet and outlet hourly air temperature profiles for buried pipes at each month

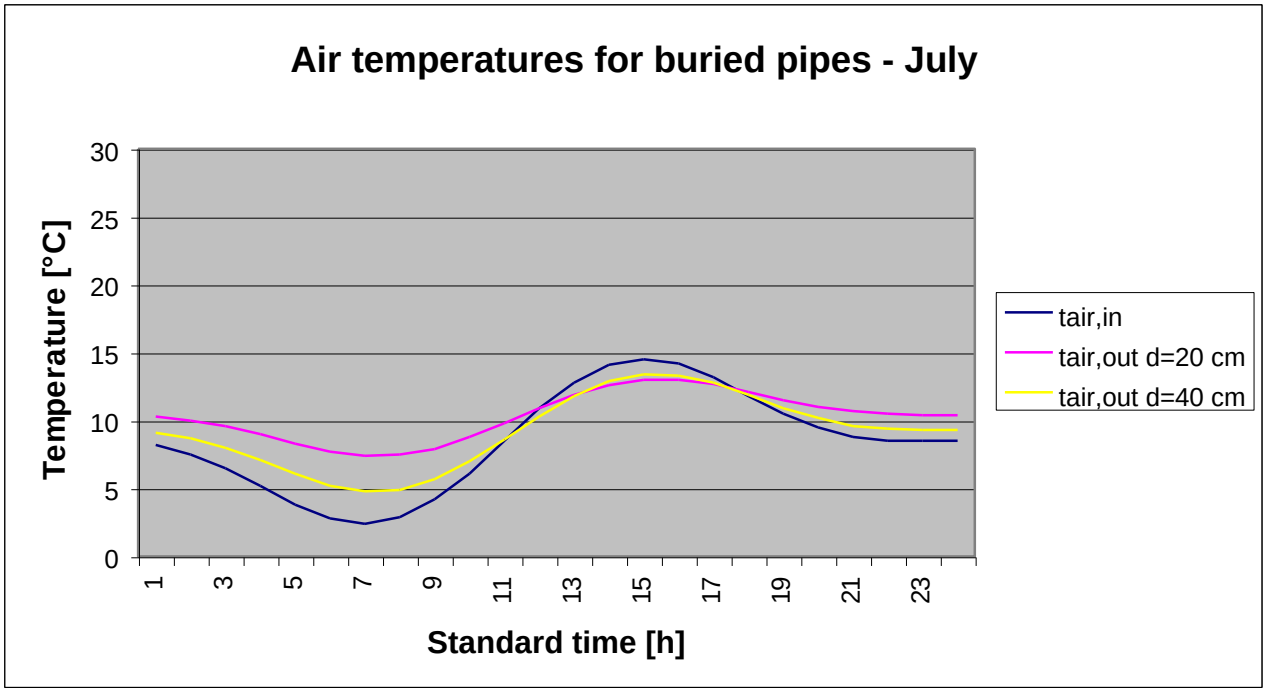

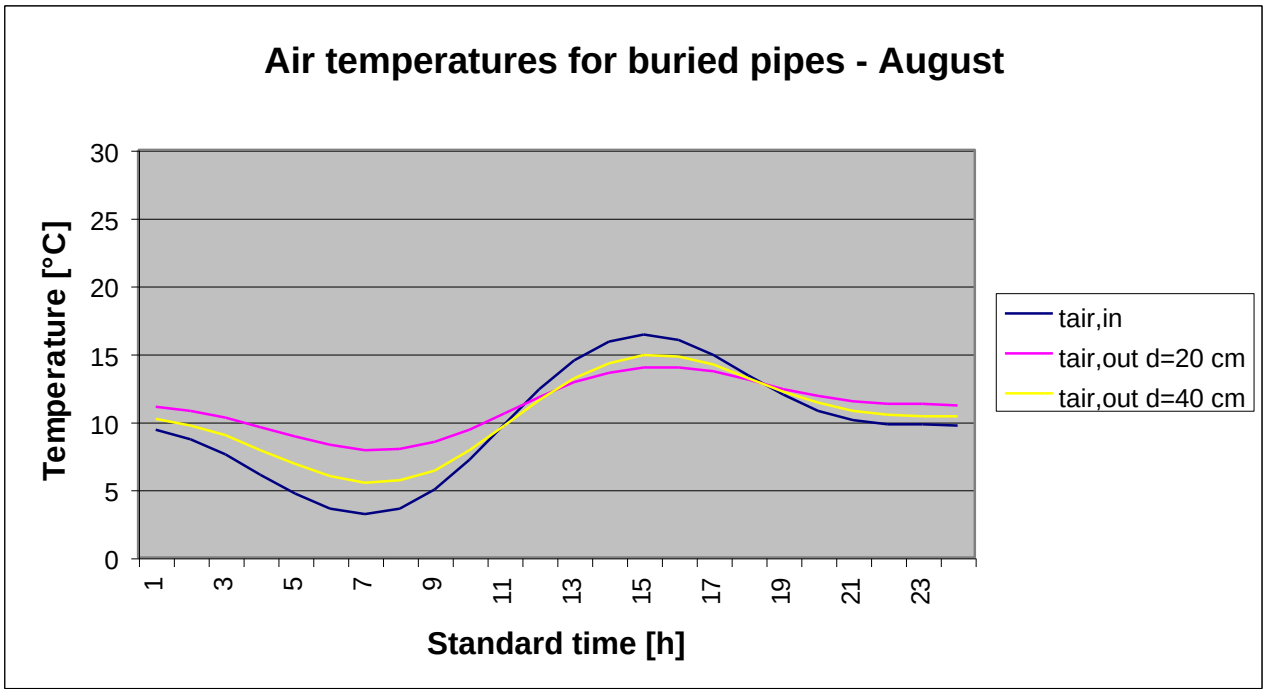

Cont.ed Fig 4 – Inlet and outlet hourly air temperature profiles for buried pipes at each month

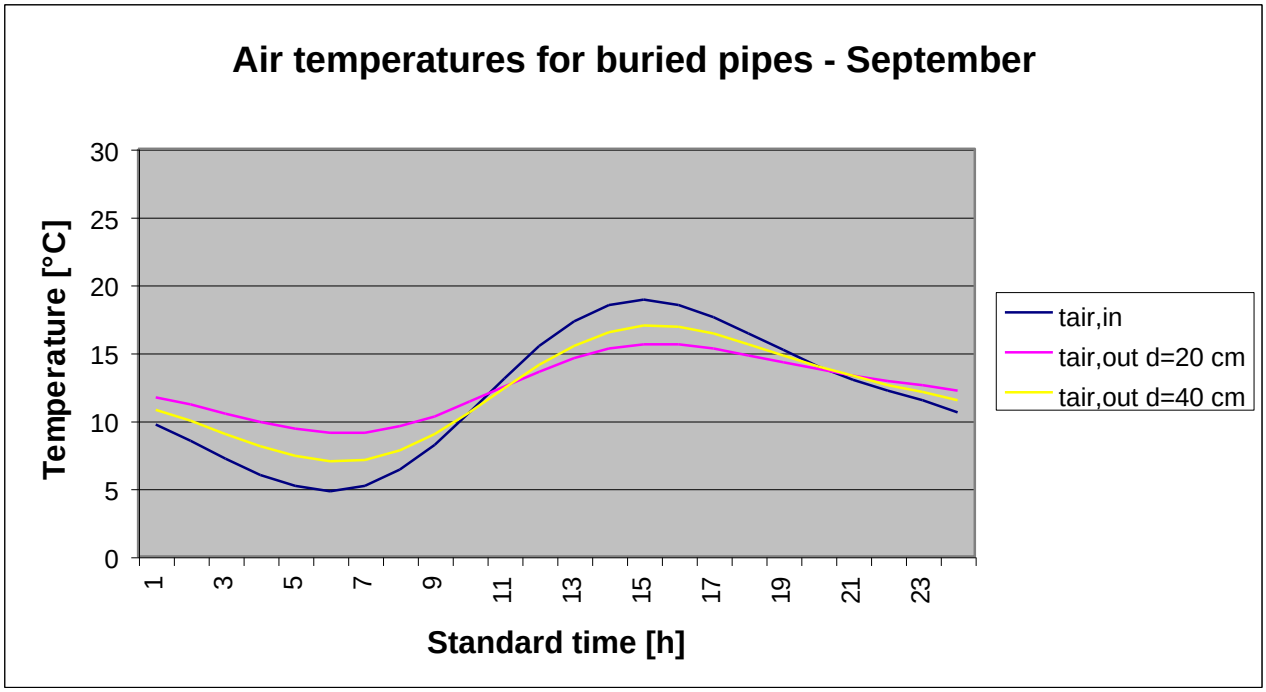

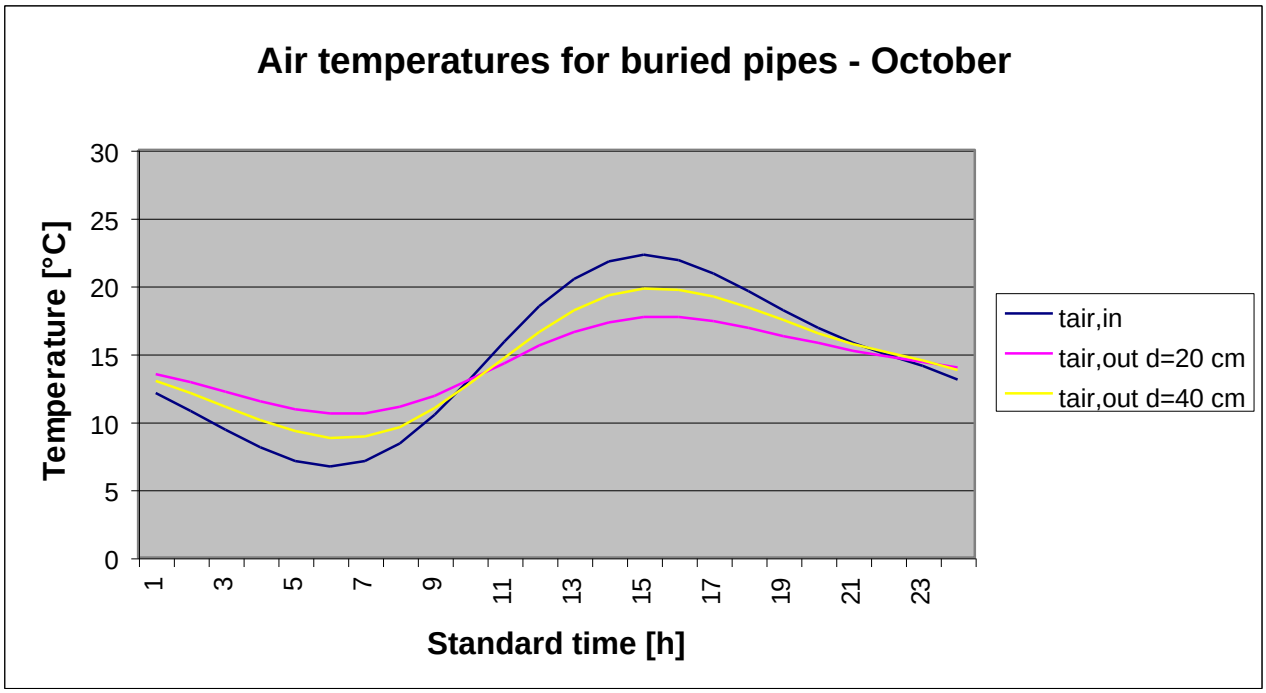

Cont.ed Fig 4 – Inlet and outlet hourly air temperature profiles for buried pipes at each month

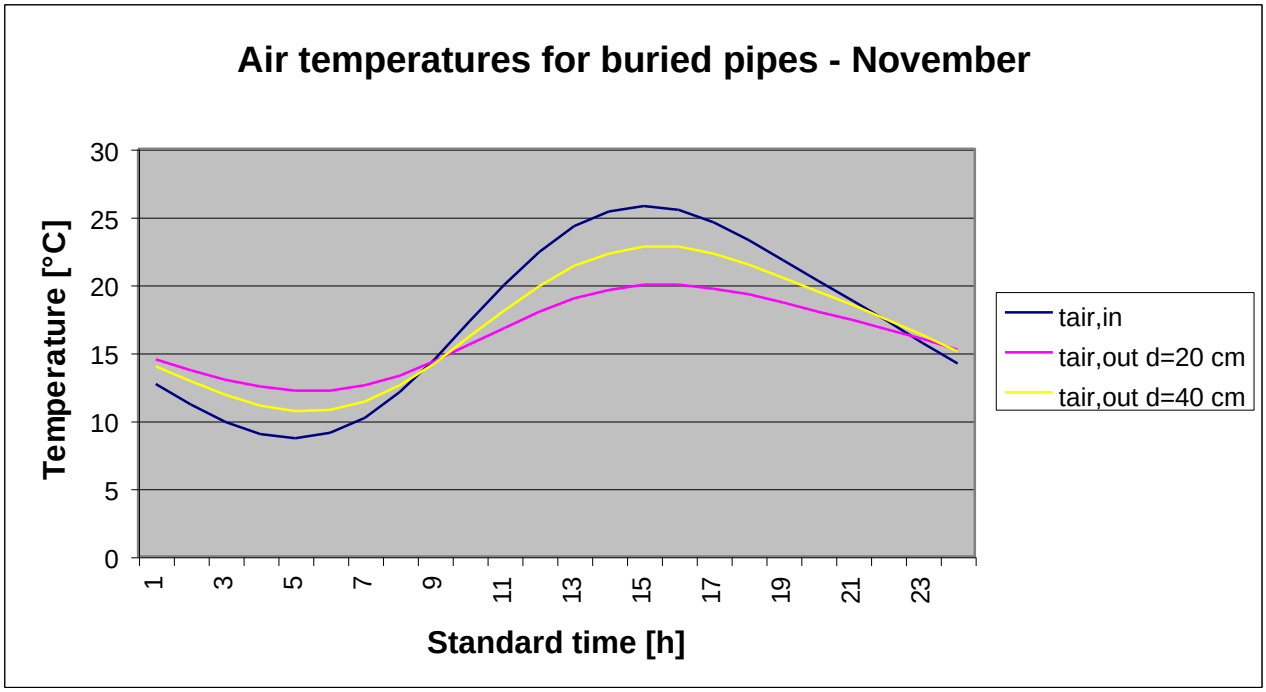

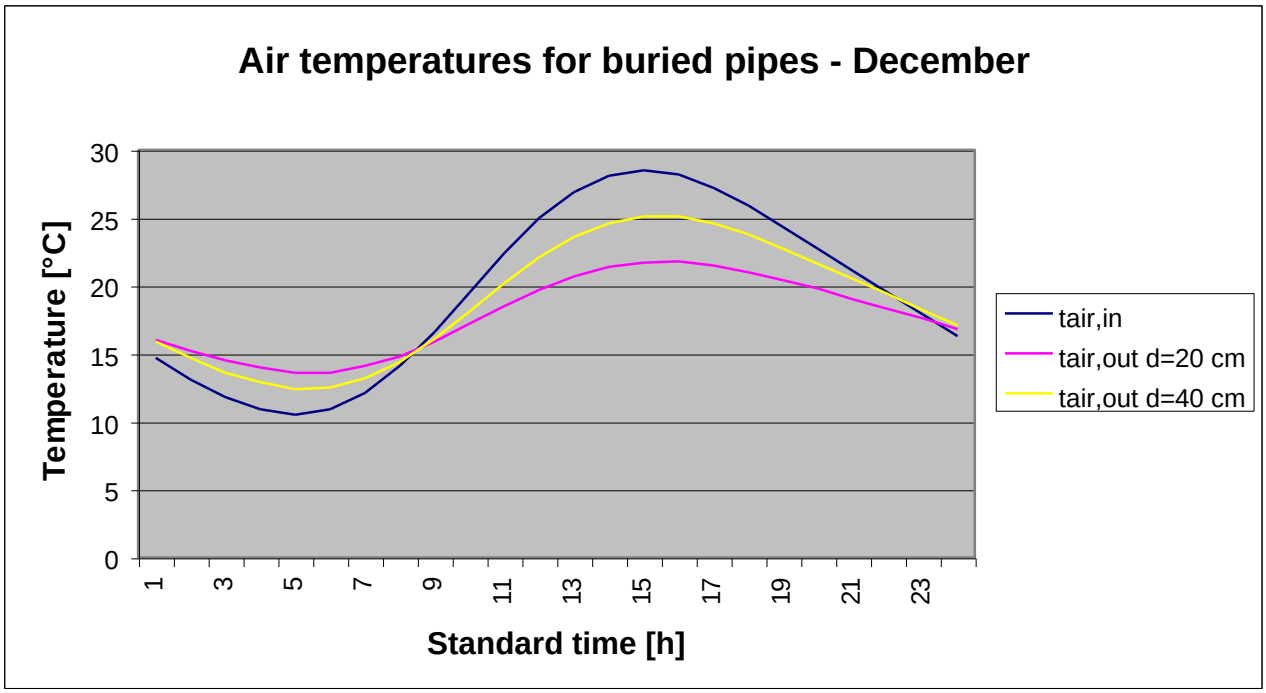

Cont.ed Fig 4 – Inlet and outlet hourly air temperature profiles for buried pipes at each month

Thermal simulations were carried out for the basis configuration with added daily ventilation through buried pipes in the system configuration described above. Both diameters, 20 and 40 cm, were checked. Tables 16a and 16b show the results.

Comparing those results to the reference ones shown in Table 11, the following comments can be made. A 70-m long buried pipe of 40-cm diameter for each ventilation module, produces 96 MWh savings (11% of REACE). In addition, a reduction of 2.4 MWh (3 % of REAHE) can be achieved. Using four 70-m long buried pipes with 20-cm diameter, potential energy savings are of 220 MWh (25 % of REACE) and 5.7 MWh (7 % of REAHE)

Heating energy savings, negligible if compared to the cooling energy savings, are referred to the first working hours of the day in the hottest months. Then, outdoor air inlet for hygienic purposes can be at a lower temperature than the minimum required for comfort while temperature of air coming from buried pipes could be higher. Though, it should be considered a possible underestimation, by the utilised thermal code, of the inertia effect due to thermal mass.

The cooling efficiency of alternative geometry configurations for buried pipes can be considered as follows, keeping unchanged material, depth, and air velocity.

- For a given length, increasing diameter leads to a decreasing of potential cooling loads reduction (quantitative effects can be drawn by interpolation of data in Table 16).
- For a given diameter, a decreasing in length leads to an almost linear decrease of the potential cooling energy savings.

While choosing buried pipe diameters different from the ones above indicated, attention should be paid to the number of pipes that are to be sufficient for the required airflow rates.

Table 16a - Annual energy (kWh): basis configuration with buried pipes – diameter 20 cm

Month	**Cooling Energy**		
	Sensible	Latent	Total
Jan	74200	5098	79298
Feb	70400	4689	75089
Mar	77100	4651	81751
Apr	53800	3142	56942
May	44000	1922	45922
Jun	34500	1373	35873
Jul	39600	1001	40601
Ago	37700	1419	39119
Sep	42500	2147	44647
Oct	59600	2668	62268
Nov	59600	3438	63038
Dec	66900	4091	70991
Total	**659900**	**35639**	**695539**

Month	**Heating Energy**		
	Sensible	Latent	Total
Jan	570	50	620
Feb	950	41	991
Mar	2280	64	2344
Apr	5490	126	5616
May	8550	222	8772
Jun	11530	314	11844
Jul	12300	452	12752
Ago	11370	315	11685
Sep	6490	195	6685
Oct	3760	167	3927
Nov	2300	99	2399
Dec	1230	82	1312
Total	**66820**	**2127**	**68947**

Table 16b - Annual energy (kWh): basis configuration with buried pipes – diameter 40 cm

Month	Cooling Energy		
	Sensible	Latent	Total
Jan	88200	5098	93298
Feb	83600	4689	88289
Mar	91600	4651	96251
Apr	63900	3142	67042
May	52300	1922	54222
Jun	40900	1373	42273
Jul	47100	1001	48101
Ago	44800	1419	46219
Sep	50500	2147	52647
Oct	70700	2668	73368
Nov	70900	3439	74339
Dec	79500	4092	83592
Total	**784000**	**35641**	**819641**

Month	Heating Energy		
	Sensible	Latent	Total
Jan	570	50	620
Feb	960	42	1002
Mar	2330	64	2394
Apr	5660	126	5786
May	8970	222	9192
Jun	12160	314	12474
Jul	12970	452	13422
Ago	11930	315	12245
Sep	6700	195	6895
Oct	3840	167	4007
Nov	2320	99	2419
Dec	1230	82	1312
Total	**69640**	**2128**	**71768**

4.2.5 *Solar air pre-heating system*

Evaluation of the energy savings obtainable by pre-heating ventilation air through solar collectors located on the roof was carried out through calculation of:

a) solar radiation on a plane tilted as the collectors' surface (Figure 5);
b) solar-air monthly-averaged hourly temperature profiles as an estimate of the air temperature within the solar collectors' air cavity (Figure 6);
c) water volume needed for storing the solar energy transferred by the collectors system during the average day of the coldest month of the year;
d) monthly energy yielded by the storage tank as a function of the differences between maximum solar-air temperature and outdoor minimum air temperature for each monthly profile;
e) ratio of this energy to the monthly reference sensible energy as an estimate of the solar contribution to the heating load of the building.

Evaluation of Air Temperature in the Solar Collectors

Operating air temperature within the air cavity of the solar collectors was evaluated using the definition of solar-air temperature, i.e., the theoretical temperature of outside air taking the effect of solar radiation into account ([9]).

The solar-air temperature t_{sa} can be derived from the following equation:

$$t_{sa} = t_e + \alpha G / h_e \quad [°C]$$

where:

t_e = outdoor air temperature [°C]
α = solar absorption coefficient (absorptance) of a surface [-]

([9]) Parameter introduced by Victor Olgyay in *Design with Climate*, Princeton University Press, New Jersey, 1969.

G = solar irradiance [W/m^2]
h_e = liminar external convective coefficient [W/m^2 °C]

Solar absorptance of the metal plate collecting surface was taken as $\alpha = 0.9$. The liminar external convective coefficient h_e was assumed to be = 11 W/m^2 °C, taking average wind conditions into account. The latter is much less than the value usually considered for external walls (23 W/m^2). This is due to the combined effect of liminar convection between collecting surface and heated air cavity and liminar convection between glass and outdoor air.

Global solar radiation hourly monthly profiles on a plane tilted as the collectors' surface are shown in Figure 5. Solar-air monthly-averaged hourly monthly temperature profiles calculated using the above equation as an estimate of the air temperature within the solar collectors' air cavity, are shown in Figure 6.

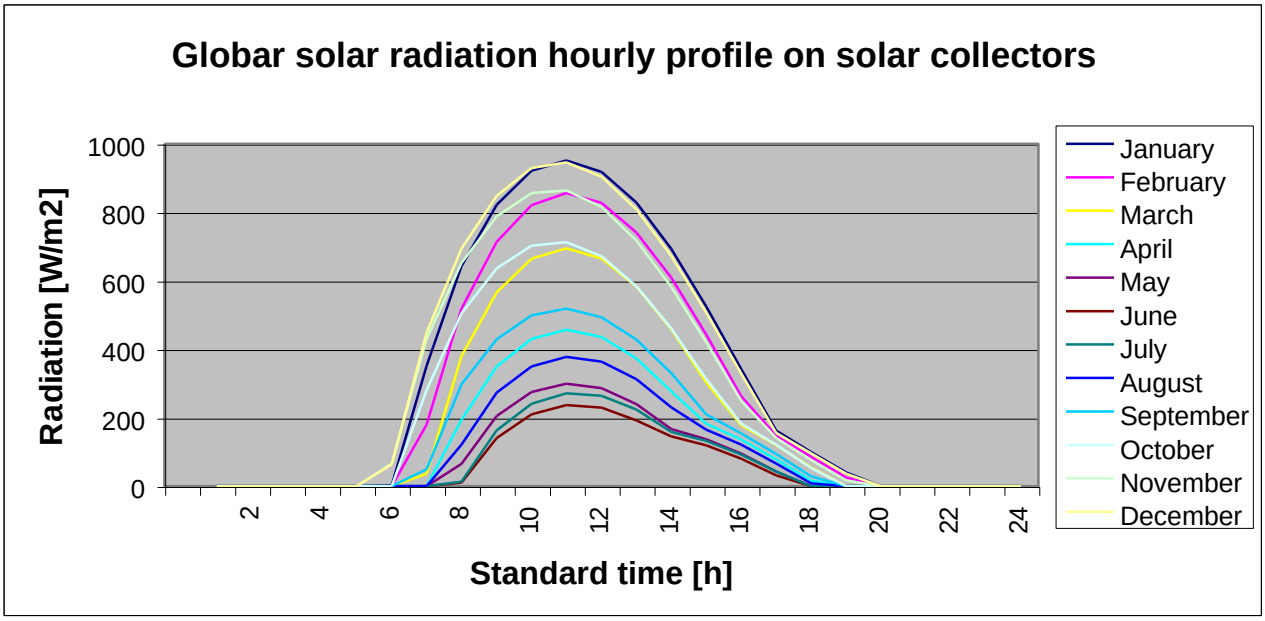

Figure 5 – Global solar radiation hourly monthly profiles
on a plane tilted as the collectors' surface

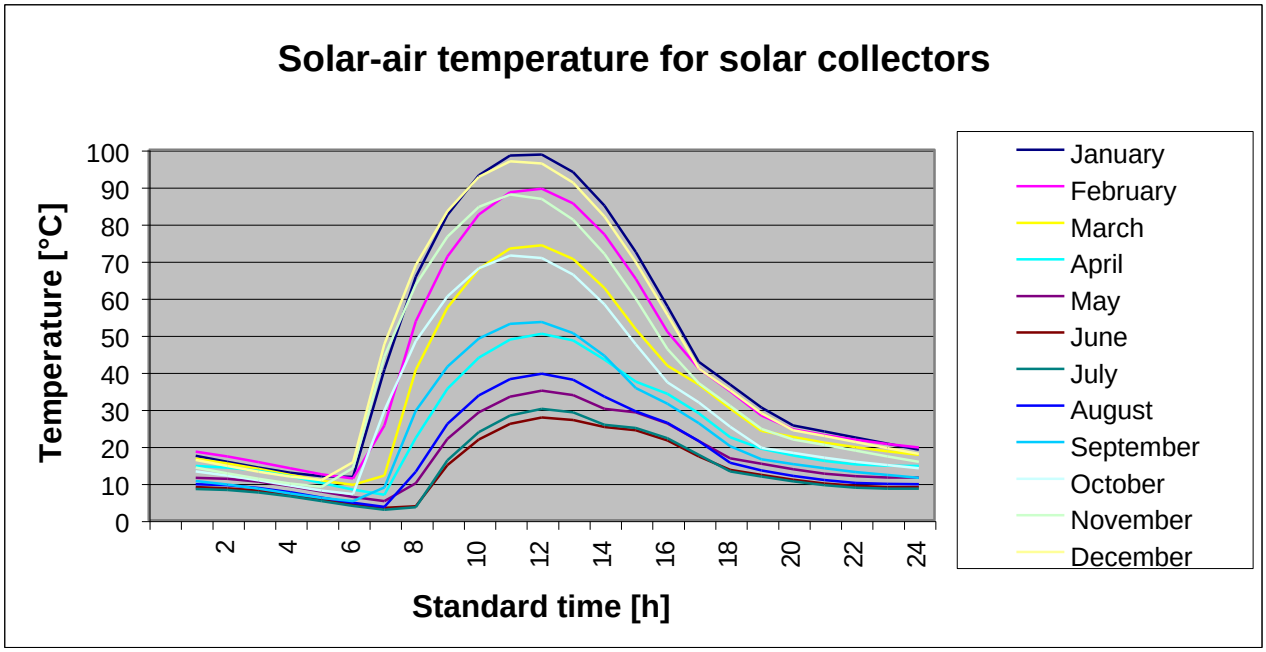

Figure 6 - Solar-air monthly-averaged hourly monthly temperature profiles as an estimate of the air temperature within the solar collectors' air cavity

Estimate of solar contribution to the heating loads

Evaluation of the available solar energy for heating was carried out in the following two steps.

a) An estimate of the daily water mass needed for storing solar collected useful energy in the month with the lowest solar irradiation (June) was made using the following equation:

$$M_{sto} = \frac{I_d \eta A_{sc}}{c_s (t_{sa(\max)} - t_{e(\min)})} [Kg]$$

Where:

I_d = Daily solar irradiation incident on a square meter of collecting surface [J/m^2](Fig. 5)
A_{sc} = Area of solar collecting surface [m^2]
η = Solar collector efficiency (50%)
c_s = Specific heat of water (4186 J/kg K)
$t_{sa(max)}$ = Maximum hourly collector solar-air temperature during a typical day of June [°C] (Fig. 6)
$t_{e(min)}$ = Minimum hourly external air temperature during a typical day of June [°C] (Table 5)

Considering daily useful solar collected energy $E_{coll} = I_d \eta A_{sc}$ = 350 kWh (0.7 kWh/m^2 × 500 m^2) or 1.26×10^9 J and $\Delta t = t_{sa(max)} - t_{e(min)}$ = 20 °C, the daily water storage mass for the whole NE wing in June is M_{sto} = 15050 kg of water (or about 15 m^3).

b) Daily available solar energy (E_{sol}) for June equals E_{coll}. In the other months, $E_{sol} = M_{sto} \times c_s \times \Delta t$ for each month. Monthly available solar energy was obtained by multiplying E_{sol} by the number of days in each month.

Daily available solar energy and Δt for each month are shown in Table 17. Values of monthly available solar energy as a contribution to sensible heating energy for each month are shown in Table 18.

Table 17 – Daily available solar energy E_{sol} and Δt for each month

Month	**Δt** [°C]	**E_{sol}** [kWh]	**Month**	**Δt** [°C]	**E_{sol}** [kWh]
January	85	1487	July	27.5	480
February	78	1365	August	36	637
March	64	1120	September	48	840
April	44	1120	October	64	1120
May	24	420	November	77	1347
June	20	350	December	84	1470

Table 18 – Monthly energy contribution of solar air pre-heating system

Month	**Sensible heating energy *(*)*** [kWh]	**Available solar contribution** [kWh]	**Total savings**	
			[kWh]	%
January	1100	46100	1100	100
February	1800	38220	1800	100
March	4180	34720	4180	100
April	9670	23100	9670	100
May	16130	13020	13020	81
June	23290	10500	10500	45
July	24600	14880	14880	60
August	21660	19750	19750	91
September	13460	25200	13460	100
October	8000	34720	8000	100
November	4030	40410	4030	100
December	2080	45570	2080	100

(*) basis configuration + pergola

4.3 Summary of energy savings

The energy savings obtainable by the above-described technologies are summarised in Tables 18 against the reference heating (Table 18a) and cooling (Table 18b) loads. As can be noted, savings are not simply added, but need to be calculated in a cascade manner.

Energy savings for two combinations of technologies – differentiated only for glazing type (single or absorbing) and buried pipes diameter (20 or 40 cm as diameter) - are also shown. Regarding heating energy, the two selected combinations are almost identical. With respect to cooling energy, the difference is more pronounced in favour of the configuration with single glass and 20-cm diameter buried pipes. However, the latter configuration with absorbing instead of single glass would perform even better.

Table 18a – Heating energy – sensible [kWh/year]

ENVIRONMENTAL CONTROL STRATEGIES	ANNUAL ENERGY					
	Reference	Increments		Savings		Total residual
		abs. val.	%	abs. val.	%	
a) basis configuration	72000					
b) *a* with overhangs		58000	80	-	-	
c_1) *a* with single glass		17000	24	-	-	
c_2) *a* with absorbing double glass		8000	11	-	-	
c_3) *a* with reflecting double glass		10000	14	-	-	
d_1) *a* with night ventilation (0,5 ACH)		1500	2	-	-	
d_2) *a* with night ventilation (3 ACH)		9000	13	-	-	
e_1) *a* with ventilation through buried pipes (radius 10 cm)		-	-	5000	7	
e_2) *a* with ventilation through buried pipes (radius 20 cm)		-	-	2500	3	
f) modified basis configuration: *b*	130000					
g) *f* with air solar collectors		-	-	102000	78	
h_1) proposed configuration: $f + c_1 + d_2 + e_1 + g$				120000	92	10000
h_2) proposed configuration: $f + c_2 + d_2 + e_2 + g$				118000	91	12000

Table 18b – Cooling energy - sensible [kWh/year]

ENVIRONMENTAL CONTROL STRATEGIES	ANNUAL ENERGY					
	Reference	Increments		Savings		Total residual
		abs. val.	%	abs. val.	%	
a) basis configuration	880000					
b) *a* with overhangs		-	-	110000	13	
c_1) *a* with single glass		-	-	53800	6	
c_2) *a* with absorbing double glass		-	-	77000	9	
c_3) *a* with reflecting double glass		-	-	120000	14	
d_1) *a* with night ventilation (0,5 ACH)		-	-	44000	5	
d_2) *a* with night ventilation (3 ACH)		-	-	176000	20	
e_1) *a* with ventilation through buried pipes (radius 10 cm)		-	-	220000	25	

e_2) *a* with ventilation through buried pipes (radius 20 cm)		-	-	96000	11	
f) a with air solar collectors		-	-	-	-	
g_1) proposed configuration: $b + c_1 + d_2 + e_1$				447000	51	433000
g_2) proposed configuration: $b + c_2 + d_2 + e_2$				380000	43	500000

The following are design criteria to be used for the SW wing, devoted mainly to collective functions, divided according to space use. No thermal analysis was performed on that part of the Consalud's Headquarters. However, most of the relative results shown above for the NE wing - in terms of potential energy savings for the various bioclimatic technologies - can be transferred to the SW wing, when the same technology applies with the due specific adaptations.

5 Bioclimatic technological indications

5.1 Cafeteria

If meals will be served during the central part of the day and not in the evening, overheating due to solar radiation should not occur because solar control is obtained through building orientation.

Considering a simultaneous average occupancy of 200 persons during operating hours, cooling loads are likely to be largely prevalent in the whole year. However, air pre-heating could be necessary in the coldest periods.

Based on those hypotheses, the following indications can be given:

a) Ventilation of the cafeteria can be realised by mechanical air exhaust through the kitchen and air supply through ductwork, or openings properly placed on the building envelope. The ventilation system has to be designed in such a way that the cafeteria be under-pressurised with respect to the entrance hall in order to avoid odour transportation. Hence, ventilators pressure head needs to be properly sized. Whichever the air supply system, non-conditioned outdoor air could be used (free-cooling); possible remaining cooling loads during operating hours, could be compensated by local units such as fan-coils to be defined within the HVAC system design development phase.
b) The above-outlined configuration can be integrated by an air supply system employing buried pipes, as in the NE wing, in order to optimise the free-cooling effect.
c) Air pre-heating in cold months – or whenever required by microclimate indoor conditions, e.g., when occupancy during operating hours is significantly reduced – can be realised by a system using solar collectors as in the NE wing. For a cafeteria, the solar technology is even more advantageous than for an office space since energy demand coincides, in time, with the period of maximum solar radiation. Orientation and tilt of solar collectors should be the same that the ones indicated for the NE wing.
d) Surface exposure of massive structures is suggested to allow for storing heat generated during operating hours as well as for mass cooling at night. As an example, stone's tiles could be applied on concrete floor slabs and counter-ceilings should not be used.

5.2 Conference hall

Occupancy of a conference hall is generally variable and its schedule difficult to be predicted.

When used in late afternoon, Consalud's conference hall can be at risk of overheating due to solar radiation incident on the SW-oriented external wall.

Analogously to what said for the cafeteria, cooling loads will be prevalent the whole year, if the conference hall is fully occupied. In the case of partial occupation, or in morning use, air pre-

heating (heating of ventilation air) as well as heating (additional introduction of air at a higher airflow rate) – in the larger hall – could be necessary.

Based on those hypotheses, the following indications can be given:

a) Shading devices should be installed on the glazed surface of the SW facade.
b) Opaque elements of the SW wall should have a high thermal inertia. Materials proposed by the designers (reconstructed stone + mortar + poured concrete) can work properly if the concrete layer is at least 15 cm thick and the stone surface of a light colour. However, an insulation layer should be included in order to reduce thermal flux due to outdoor-indoor temperature difference.
c) Buried pipes could be potentially useful also for this space while solar collectors appear to be less appropriate (useful only when the conference hall is occupied scarcely, or in the morning).
d) Considering the tendency of a flexible microclimate control in meeting rooms and conference halls (also for PR reasons), a back-up "traditional" HVAC system would be probably helpful. This system would control the majority of indoor microclimate parameters with the exclusion of the ones depending on envelope interaction.

5.3 Top Floor

The space at the top floor, half used as a call centre and the other half for offices, has a similar thermal behaviour as the NE wing. The same above-described bioclimatic technologies can, therefore, be applied.

In particular, the ventilation system suggested for the NE wing – with pre-cooling through buried pipes and pre-heating by solar collectors – could be extended to the top floor of the SW wing. However, additional space should be found to locate both solar collectors and buried pipes with relevant air handling units.

5.4 Entrance hall

The entrance hall is a typical *atrium* space with heating loads during the cold season and cooling loads in warm and hot months, when serious overheating risks may occur due to the northern exposure of a large part of the glazed wall.

From a plant standpoint, the optimal solution for heating could be a floor-imbedded water-pipes radiant system usable also in the hot season for basic cooling.

The following bioclimatic criteria can be suggested:

a) The proposed radiant floor heating system work very well in combination with a stack effect ventilation strategy obtainable through openings located at the bottom and at the top of the glazed wall. This strategy, which needs to be minimised during winter, operates for both indoor air quality and indoor cooling (free cooling). Opening should be, possibly, controllable in relation to indoor microclimate conditions.
b) A movable-shading device installed, possibly, on the external side of the glazed wall would be useful. It would allow for keeping maximum winter solar irradiation by choosing clear glass (necessarily double) while avoiding possible summer overheating.

CONCLUSIONS

An optimal thermal and energy performance should be obtained in the whole Consalud's headquarters building by following the above-indicated design advises as well as introducing the proposed bioclimatic technologies, summarised as follows:

- Linear building form for office spaces
- Building orientation of 20° from North towards East
- 6 m deep overhanging pergola on the four sides of the NE wing
- Double glazing with external absorbing pane for the northwards and southwards walls of the NE wing as well as for SW-oriented windows of the SW wing
- Thermal mass for floor slabs as well as SW wall of the SW wing
- Night ventilation of floor slabs
- Free-cooling when appropriate
- Cooling by ventilation through buried pipes
- Heating by ventilation through solar collectors located on the roof of the NE wing
- Stack ventilation of entrance hall

However, extremely important for an actual achievement of the expected energy savings as well as comfort conditions, is a careful HVAC design development. In that phase, particular attention should be paid to the airflow control and distribution system in order to respond to a wide range of varying indoor microclimate requirements.

It is suggested that an airflow and thermal monitoring automatic system be installed in order to check the performance of the whole HVAC system as well as of the single bioclimatic technologies. Records of airflow rates, air temperature, and humidity should be measured at the most significant points of the ventilation ductwork, i.e., upstream and downstream the main thermal conversion and distribution devices (solar collectors, buried pipes, room supply ducts, air handling units, solar water tank and water-air heat exchangers), as well as in various typical spaces. If the monitoring system were installed during the HVAC construction phase, costs would be reduced.

Prof. Arch. Mario Grosso

Turin, December 3, 1998.